Digital Comprehensive Summaries of Uppsala Dissertations
from the Faculty of Science and Technology 2362

Visual and magnetic detection of antimicrobial resistance genes using nanoparticles and isothermal amplification

DARÍO SÁNCHEZ MARTÍN

ACTA UNIVERSITATIS
UPSALIENSIS
2024

ISSN 1651-6214
ISBN 978-91-513-2033-5
urn:nbn:se:uu:diva-522171

UPPSALA
UNIVERSITET

Dissertation presented at Uppsala University to be publicly examined in lecture room Sonja Lyttkens, Ångströmlaboratoriet, Lägerhyddsvägen 1, Uppsala, Monday, 25 March 2024 at 09:00 for the degree of Doctor of Philosophy. The examination will be conducted in English. Faculty examiner: Associate Professor Mahiar Hamedi (KTH).

Abstract

Sánchez Martín, D. 2024. Visual and magnetic detection of antimicrobial resistance genes using nanoparticles and isothermal amplification. *Digital Comprehensive Summaries of Uppsala Dissertations from the Faculty of Science and Technology* 2362. 80 pp. Uppsala: Acta Universitatis Upsaliensis. ISBN 978-91-513-2033-5.

Antibiotic resistance is becoming an increasing concern, necessitating new ways to diagnose and treat it rapidly and accurately. One proposed solution is the use of nucleic acid amplification tests, capable of detecting resistance in just a few hours, as opposed to the several days that traditional testing methods may require. One concept for such a test involves the volume-amplified magnetic nanobead detection assay (VAM-NDA), which combines rolling circle amplification (RCA), an isothermal amplification method, with magnetic nanoparticles (MNPs) for the detection of the RCA products.

In this thesis, improvements have been made to the VAM-NDA. Coupling of RCA products with microparticles allowed a greater hydrodynamic increase of the MNPs when bound to these products, facilitating the detection of shorter products. Moreover, circle-to-circle amplification (C2CA) was performed, a technique comprising two RCA reactions, increasing the sensitivity of the assay and leading to a 1 attomole limit of detection.

Optimization of several reaction parameters has allowed for increased sensitivity. Of highest relevance are the changes made to the length of padlock probes, oligonucleotides used for target recognition. These changes resulted in faster amplification. Equally important is the work conducted on phi29 DNA polymerase. Different manufacturers and mutants of this enzyme were tested, resulting in an improved and faster amplification. However, a previously undiscovered feature of this enzyme was also investigated, where phi29 amplification is competitively inhibited by the presence of ssDNA oligonucleotides, regardless of whether digestion of those is possible or not.

Finally, a novel detection method for RCA products was developed, where nanoparticles were made to aggregate with the DNA products, resulting in aggregates visible to the naked eye. This method was further optimized, and integrated with C2CA, as well as substituting MNPs for coloured polystyrene nanoparticles. The result is a fast assay that can detect down to 100 zeptomoles of target DNA visually, in less than two hours. The use of coloured nanoparticles also allowed multiplexing using two sets of nanoparticles with different colours, and two targets were detected in a single sample.

In conclusion, this thesis brings a DNA detection method one step closer to its use in the identification of antimicrobial resistance. The improvements to VAM-NDA and magnetic detection, advances on padlock probe design, the discovery of a novel behaviour of phi29 DNA polymerase, and the potential for naked-eye detection and multiplexing are of high relevance for future basic and translational research.

Keywords: DNA amplification, isothermal amplification, visual detection, nanoparticles, VAM-NDA, rolling circle amplification, phi29 DNA polymerase, padlock probes.

Darío Sánchez Martín, Department of Materials Science and Engineering, Nanotechnology and Functional Materials, Box 35, Uppsala University, SE-751 03 Uppsala, Sweden.

ISSN 1651-6214
ISBN 978-91-513-2033-5
URN urn:nbn:se:uu:diva-522171 (http://urn.kb.se/resolve?urn=urn:nbn:se:uu:diva-522171)

“People who fail to regard the truth seriously in small matters,
cannot be trusted in matters that are great.”
-Albert Einstein.

List of Papers

This thesis is based on the following papers, which are referred to in the text by their Roman numerals.

I. **Sánchez Martín, D**.*, Oropesa-Nuñez, R.*, Zardán Gómez De La Torre, T. (2021) Evaluating the performance of a magnetic nanoparticle-based detection method using circle-to-circle amplification. *Biosensors*, Vol. 11, no 6, article ID 173.

II. **Sánchez Martín, D**., Oropesa-Nuñez, R., Zardán Gómez De La Torre, T. (2021) Formation of Visible Aggregates between Rolling Circle Amplification Products and Magnetic Nanoparticles as a Strategy for Point-of-Care Diagnostics. *ACS Omega* 6: 32970–32976.

III. **Sánchez Martín, D**., Wrande, M., Sandegren, L., Zardán Gómez de la Torre, T. (2022) Naked-eye detection of antibiotic resistance gene *sul1* based on aggregation of magnetic nanoparticles and DNA amplification products. *Biosens. Bioelectron. X* Vol. 12, article ID 100277.

IV. **Sánchez Martín, D**., Oropesa-Nuñez, R., Zardán Gómez De La Torre, T. (2023) Rolling Circle Amplification on a Bead: Improving the Detection Time for a Magnetic Bioassay. *ACS Omega*, Vol. 8, no 4, p. 4391-4397.

V. **Sánchez Martín, D**., Li, T. Wrande, M., Sandegren, L., Tian, B., Strømme, M., Zardán Gómez de la Torre, T. (2023). Reduced amplification by phi29 DNA polymerase in the presence of unbound oligos during rolling circle amplification. *Accepted in Biosens. Bioelectron. X*.

VI. **Sánchez Martín, D**., Strømme, M., Zardán Gómez de la Torre, T. (2023). Sensitive multiplex visual detection of DNA targets using colored polystyrene nanoparticles and circle-to-circle amplification. *Manuscript.*

*= Authors contributed equally to this work.

Reprints were made with permission from the respective publishers.

Author contributions

The author's contributions to the Papers included in this thesis are as follows:

Paper I: I performed the specificity testing, and took part in the analysis of the results, and writing of the manuscript.

Paper II: I took part in the planning of the study, developed the methodology, and performed most of the experimental work, analysis of data, and writing of the manuscript.

Paper III: I took part in the planning of the study, developed the methodology, and performed most of the experimental work, analysis of data, and writing of the manuscript.

Paper IV: I took part in the planning of the study, and performed the experiments with spiked samples testing the specificity, analysis of data, and writing of the manuscript.

Paper V: I planned the study and methodology, performed most of the experimental work, analysis of data, and writing of the manuscript.

Paper VI: I planned the study and methodology, performed the experimental work, analysis of data, and writing of the manuscript.

Other works

Conferences:

Sánchez Martín, D., Wrande, M., Sandegren, L., Zardán Gómez de la Torre, T. Circle to circle amplification for detection of antibiotic resistance genes. Uppsala Antibiotic Days: a multidisciplinary conference, 2022, p. 37. *Oral presentation.*

Sánchez Martín, D., Zardán Gómez de la Torre, T. Development of a naked-eye DNA detection method based on magnetic nanoparticles. 7th International Conference on Multifunctional, Hybrid and Nanomaterials, 19-22 Oct 2022, Genoa, Italy, 2022. *Poster presentation.*

Sánchez Martín, D., Zardán Gómez de la Torre, T. Investigation of rolling circle amplification product and their aggregation with magnetic nanoparticles – Visual detection of antibiotic resistance genes. 7th International Conference on Bio-sensing Technology, 2022. *Poster presentation.*

Sánchez Martín, D., Wrande, M., Sandegren, L., Zardán Gómez de la Torre, T. Controlled aggregation of colored nanoparticles and DNA amplification products for visual detection of antimicrobial resistance. 33rd Anniversary World Congress on Biosensors, 2023. *Poster presentation.*

Sánchez Martín, D., Wrande, M., Sandegren, L., Zardán Gómez de la Torre, T. Fast, specific and visual detection of antibiotic resistance genes through isothermal DNA amplification using minimal equipment. The PhD AMR One Health mini-conference, 2023. *Poster presentation.*

Sánchez Martín, D., Wrande, M., Sandegren, L., Zardán Gómez de la Torre, T. Nanoparticle-based bioassay for visual detection of antibiotic resistance genes – current work and future perspectives. #RSCPoster Twitter poster conference, 2023. *Poster presentation, online.*

Sánchez Martín, D., Wrande, M., Sandegren, L., Zardán Gómez de la Torre, T. Visible aggregation of nanoparticles and DNA for out-of-laboratory testing of antimicrobial resistance. MedTech Science and Innovation Day, 2023. *Oral presentation.*

Contents

Abbreviations

AC	alternate current
AI	artificial intelligence
AMR	antimicrobial resistance
ATP	adenosine triphosphate
Au	gold
BNF	bionized nanoferrite
C2CA	circle-to-circle amplification
CB	capture bead
CO	capture oligonucleotide
COVID-19	coronavirus disease 2019
DNA	deoxyribonucleic acid
dNMP	deoxynucleotide monophosphate
dNTP	deoxynucleotide triphosphate
DO	detection oligonucleotide
dsDNA	double-stranded deoxyribonucleic acid
eccDNA	extrachromosomal circular DNA
LAMP	loop-mediated isothermal amplification
LOD	limit of detection
MDA	multiple displacement amplification
MNP	magnetic nanoparticle
NAAT	nucleic acid amplification technique
NC	negative control
PCR	polymerase chain reaction
Pi	inorganic phosphate
PLP	padlock probe
POC	point of care
PPi	inorganic pyrophosphate
PS-NP	polystyrene nanoparticle
qPCR	quantitative polymerase chain reaction
RCA	rolling circle amplification
RFLP	restriction fragment length polymorphism
RNA	ribonucleic acid
RO	restriction oligonucleotide
RPA	recombinase polymerase amplification
SD	standard deviation

SPR	surface-plasmon resonance
ssDNA	single-stranded deoxyribonucleic acid
UV	ultraviolet
UV-vis	ultraviolet-visible
VAM-NDA	volume-amplified magnetic nanobead detection assay
χ''	imaginary part of the complex magnetic susceptibility

1. Introduction and aims

There are known unknowns. In healthcare and medical science, symptoms do not provide the full picture of a disease or condition. When a person, animal, or plant is sick, it is often the known unknowns that make treatment hard. Is a disease viral, fungal, or bacterial? Is the pathogen sensitive to a specific medication, or resistant to it? We are perfectly aware of these important questions, and yet, they can be hard to answer, especially in time for an efficient treatment of disease.

Common diagnosis of a disease is usually done in hospitals by cultivating the microorganism to identify it. However, that can be quite slow, taking up to 3 days in many cases. In the last few decades, a new concept has taken root in how we can tackle this problem: diagnostic tests. These are quicker methods for identifying the type and characteristics of pathogens in simpler tests. Many strategies are used to design said tests, as the goal is to have fast, accurate, and cheap diagnoses. However, it is hard to find a single test that combines all the mentioned traits.

Although tests aim to detect different parts of the pathogens or indicators of their presence, one of the most common techniques is nucleic acid amplification techniques (NAATs). As all pathogens have some DNA or RNA, and their identity and characteristics are encoded in specific fragments of such molecules, nucleic acids are a great target for diagnostic tests.

This doctoral thesis aims to improve, streamline, and optimize a nucleic acid detection technique using nanoparticles to work optimally in biological samples. This technique provides fast results, in under 2 hours, can be used to detect specific DNA fragments of relevance, and provides visual results, which means that less equipment is needed.

The aims of each specific paper are listed below

Paper I: This paper aims to evaluate the feasibility of circle-to-circle amplification for clinical diagnostics, using magnetic nanoparticles for detection. It involves comparison with rolling circle amplification and investigation of the stability of functionalized magnetic nanoparticles.

Paper II: This paper aims to develop a novel DNA detection method, based on the aggregation of DNA and magnetic nanoparticles, is coupled with the

rolling circle amplification technique to allow visual detection of DNA in samples, without the need for readout instrumentation.

Paper III: The objective of this work is to optimize the assay and aggregation-based detection, presented in Paper II, to work with circle-to-circle amplification. It involves testing the method with biological samples, showing the feasibility of visual detection of antibiotic resistance gene *sul1*.

Paper IV: This work aims to explore the possibility of performing rolling circle amplification on the surface of microbeads. The objective is to preserve the substantial size of the products while minimizing the amplification time, thereby reducing the overall assay time.

Paper V: This paper aims to investigate a previously undiscovered competitive inhibition of phi29 DNA polymerase in amplification reactions, occurring specifically between extendable and digestible DNA.

Paper VI: The objective of this study is to optimize the circle-to-circle amplification technique and aggregation-based detection for increased sensitivity. It includes testing the aggregation using coloured polystyrene nanoparticles. Additionally, the study allows visual detection of two DNA targets within a single reaction.

1.1. Antibiotic resistance and the need for detection

As previously mentioned, this thesis focuses on the detection of nucleic acids, which can be used to detect and characterize various pathogens. It is important to emphasize the fact that the groundwork laid here has the potential for different applications in medical, agricultural, and environmental areas. However, the tests performed in the presented papers are primarily intended to identify antimicrobial resistance (AMR) in bacteria. The reason for this is that antibiotic resistance is a growing worldwide problem. This is caused by the increase in resistance to currently available antibiotics, due to overprescription and misuse, coupled with the lack of new drug discoveries in the antibiotic field[(1)]. Untimely and inaccurate treatment of patients with bacterial infections leads to huge health and economic issues. As of 2023, the cost of antimicrobial resistance in Europe adds up to €1.1 billion in healthcare costs alone, with 100 people dying daily because of AMR in Europe in 2020[(2)]. Moreover, it is estimated that the total cost due to AMR between 2014 and 2050 will reach $100 trillion worldwide if current trends continue, potentially causing 10 million deaths in 2050 alone[(3)]. Alarmingly, over 50% of antibiotic treatments are started without any knowledge of possible resistance[(4)]. Thus, there is a critical need for accurate and fast detection of resistance.

1.1.1. Detection strategies

Different methods to determine antibiotic resistance have existed for a long time. But as our technology improves so does our capability for detection. The most common detection method for antibiotic resistance starts by obtaining a sample, determining the species using staining and microscopy, and then growing the bacteria in a culture[4]. In this culture, antibiotics are added to see if the bacteria can grow with the theoretically harmful molecules. This is usually done in the traditional disk diffusion test[5], but other methods are available[6]. This process demands a substantial amount of laboratory equipment and it can take up to 3 days[4], especially in the cases of multiresistant bacteria[7], which usually grow slower.

Antibiotic resistance is in most cases caused by antibiotic resistance genes, which encode proteins that modify, excrete, or destroy the antibiotic molecules to reduce or negate the harmful effects on the bacterial cell[7]. Detection of the genes can occur before the expression of proteins, which makes antibiotic resistance gene detection a great pre-treatment asset, but other tests are available to determine the presence of the proteins or the ability of the bacteria to grow in the presence of antibiotics[6,8]. While these tests are not to be underestimated and can be a great tool, the focus of this work is on the detection of antibiotic resistance genes. Figure 1 shows the difference between the classic laboratory pipeline for the detection of antibiotic resistance versus the antibiotic resistance gene detection methods.

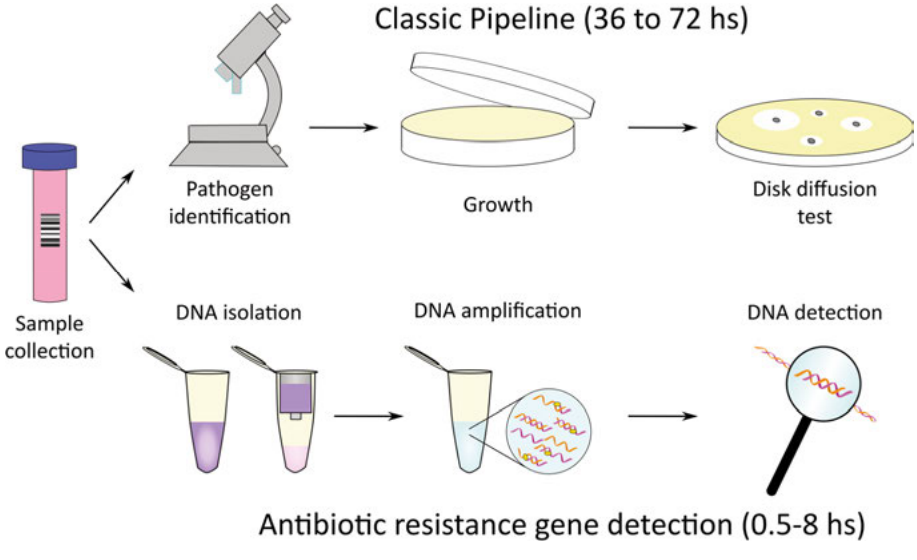

Figure 1: Illustration of the classic antibiotic resistance detection methods vs the new gene detection methods.

1.2. Biosensors and bioassays

The specific definitions of a biosensor and bioassay are not clear, and there is still no accurate consensus on how to define them. Roughly put, a biosensor is a device with a biological sensing element that produces a signal in the presence of a given molecule[9]. The signal is picked up by a transducer and an output signal is generated. A bioassay is a test to determine certain characteristics of a sample, in which a biological component is used[10]. A biosensor and bioassay may serve the same purpose, but one is a device that performs a task, and the other is a test that needs to be performed. The differences and similarities of biosensors and bioassays are represented in Figure 2.

A biosensor, in many cases, is simply a device that performs a bioassay and generates an output signal. This thesis deals with the development and improvement of a bioassay, although the long-term goal has always been to integrate it into a biosensor or a microfluidic test device. A microfluidic test device is a small, automated device that carries out reactions on its own. It only needs the introduction of a sample at a starting point, after which the sample travels through the channels in a pre-set form. Reagents can be delivered with the sample or preloaded in the device in dried form. Human supervision is not required to carry out the reactions[11].

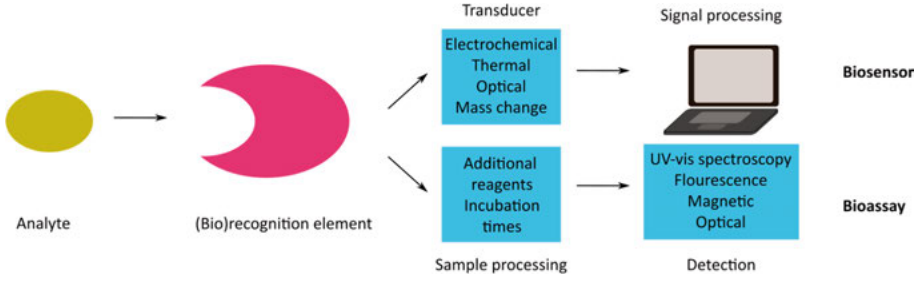

Figure 2: A basic representation of biosensors and bioassays. Both are designed to detect an analyte or a characteristic of one. Through a recognition element, which is biological for biosensors and usually for bioassays as well, there is a measurable change. In biosensors, a transducer produces a signal upon recognition, which is processed and displayed. In bioassays, other reagents may be used and normally incubation times are required. An instrument is finally used to detect changes in the recognition element or downstream steps resulting from the recognition. If the recognition element is not biological, other biological components are used downstream for it to qualify as a bioassay.

1.2.1. Point of care testing

Regardless of the type of test chosen, whether it be classic or antibiotic resistance gene detection, both may require lots of equipment, as well as trained personnel and clean conditions. Nowadays there is a push to move past the need for centralized laboratories and move testing closer to the patient, using

so-called point of care (POC) testing. This means testing that can be performed at the bedside of a patient in a hospital, in a doctor´s clinic, or even at home by the patient [12]. Such types of testing require devices that can run complex tests on their own, usually using a biosensor. Alternatively, a bioassay can be performed in a small testing device, often disposable, like in the case of the COVID-19 testing using lateral flow immunoassays.

In specific cases of bacterial infections, practitioners often need to prescribe antibiotics without conducting laboratory tests before treatment. For instance, in urgent situations, such as sepsis, waiting for lab results is not an option. Additionally, in rural areas and developing countries, the absence of nearby laboratories is a great challenge. These obstacles push the science towards simpler, cheaper, and faster assays and devices that can be manufactured in advance and miniaturized as much as possible[13]. These have been some of the issues driving the work performed in this thesis.

2. DNA amplification

DNA detection can be accomplished in several ways. Cutting-edge technology makes it possible to detect DNA without any amplification, for example by some forms of sequencing, or extremely sensitive colorimetric or fluorescence-based methods[14]. However, when we look to detect a small fragment of a specific sequence, amplification is usually required before the detection step.

DNA amplification can be done in many ways, but usually requires some similar components. Namely, it needs an enzyme that carries out a polymerization reaction of a specific fragment. The specific fragment also needs to be recognized by something, usually a complementary sequence. This is also required for amplification, as most polymerases require dsDNA to initiate the polymerization.

However, once we have covered these requirements, amplification can be performed in several ways, which are described below.

2.1. Thermal cycling vs isothermal amplification

The most common DNA amplification technique is the polymerase chain reaction, or PCR[15,16,17]. This technique has become the gold standard because it provides exponential amplification, meaning that it can generate a lot of DNA copies from a few copies of a target. PCR is based on thermal cycling, changing the temperature of the reaction many times[18]. This is because once the duplication of the target has occurred, a denaturalization step at high temperatures (usually around 95 ˚C) is used to separate the product and template, allowing both to become templates for subsequent amplifications[18]. For this, PCR requires a polymerase that can perform amplification at high temperatures and withstand 95 ˚C while remaining viable. On the other hand, PCR has many disadvantages, such as issues with false positives and negatives[19], but also the requirements for trained personnel and the need for a thermal cycler, a bulky and costly machine that usually can only be found in laboratories[20].

To bring DNA amplification and detection to other settings, we find an alternative in isothermal amplification[20]. This is done by polymerases working at a single temperature. In many cases, this can be room temperature, but otherwise, using a simple heater to bring the samples to any desired

temperature can easily be accomplished[21]. Additionally, such heaters are much cheaper and easier to use than thermocyclers. Isothermal amplification often relies on polymerases capable of strand displacement[22,23]. While thermocycling allows for heat to separate the template and product DNA strands, in isothermal amplification that does not happen, so a different way to separate them or create new templates is required. Strand displacement is a feature of some polymerases that allows them to separate dsDNA encountered downstream while performing amplification. A few examples of isothermal amplification techniques are rolling circle amplification (RCA)[24,25], loop-mediated isothermal amplification (LAMP)[26], recombinant polymerase amplification (RPA)[27], or multiple strand displacement (MDA)[28].

A simple schematic of the instrument required for PCR and thermal cycling schedule can be found in Figure 3, panel A, while the representation of a simple heater and the temperature control for isothermal amplification can be found in panel B of the same scheme.

2.2. Linear vs exponential amplification

A very important part of an amplification technique is the quantity of product it generates, as usually, the detection of DNA requires a relatively large quantity of DNA. An amplification that generates more total DNA will provide a more sensitive method, with less starting DNA required for detection. A key mechanism for generating a lot of DNA copies is if the method can create more templates or target DNA. DNA polymerases provide amplification at a given rate, but how many polymerases can act is mostly dependent on how many targets can be bound and amplified simultaneously. If that number can increase during the reaction, it is an exponential amplification method. If it cannot, it will be a linear amplification method. The difference can be seen in Figure 3, panels C and D.

While exponential amplification is best for sensitivity, it is not always the best for specificity[29]. Once a mistake is made and a non-target DNA fragment is amplified, the exponential reaction will generate more and more products, resulting in a false positive[29].

Exponential amplification is usually achieved by adding a synthetic primer that can bind to the products of a first, linear, amplification. Doing so always results in mostly dsDNA products, while linear amplification can result in either ssDNA or dsDNA products depending on the specific method and setup. Most methods aim for exponential amplification, and this is the usual case of PCR, LAMP, and RPA. RCA has the potential to achieve exponential amplification[30,31], but often RCA is performed without the required primers for exponential amplification, and generates ssDNA products[32,33,34].

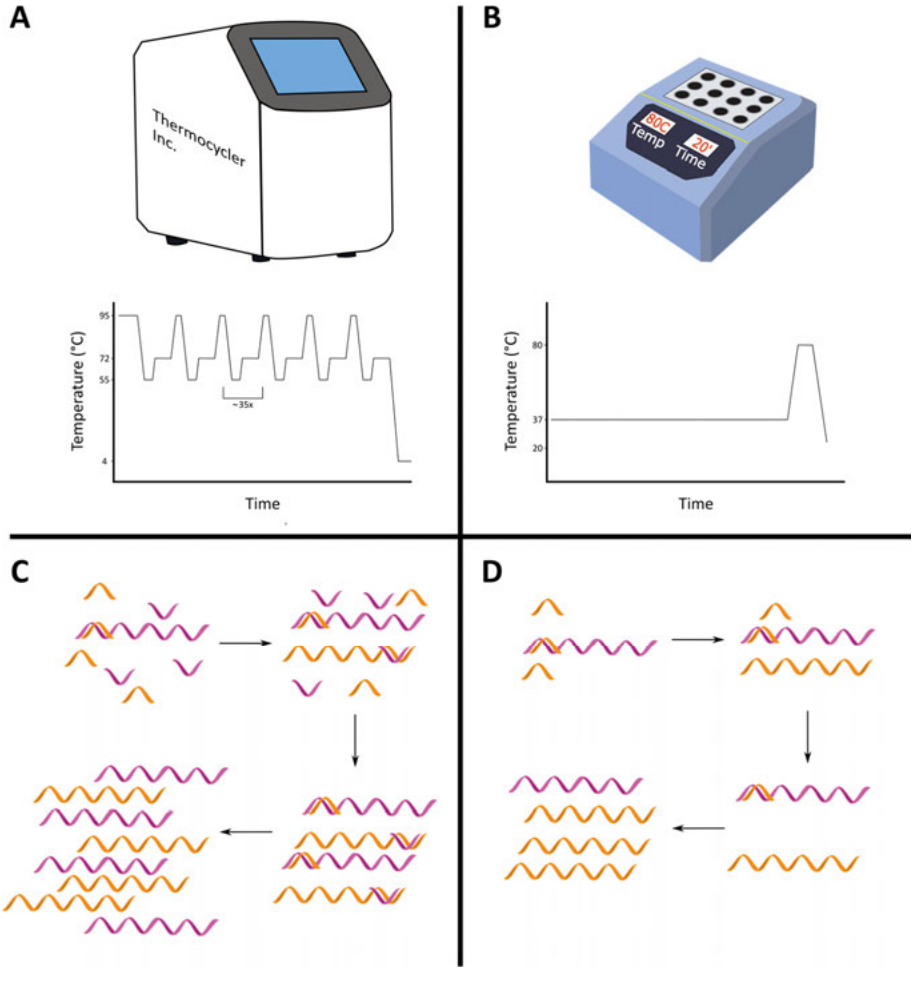

Figure 3: Types of amplification. Main features of **A:** thermal cycling, where a thermocycler is used to change temperatures many times during the reaction. **B:** isothermal amplification, where a simple heater can be used as the temperature is constant throughout most of the reaction. **C:** exponential amplification, where a single template generates products that can be used as templates with complementary primers, for exponential amplification. **D:** linear amplification, where a single template and primer generate products one at a time.

2.3. Rolling circle amplification and circle-to-circle amplification

RCA takes its name from rolling circle replication, a type of DNA replication used by bacteria and viruses to copy circular DNA elements. In RCA, a circular template is used for amplification by a polymerase with high strand

displacement, that polymerizes long ssDNA products of concatenated copies of the complementary sequence to the circular template[24,25].

RCA in diagnostics is usually performed with padlock probes (PLPs), linear ssDNA oligos of around 40-120 nt that bind complementary to a target of choice through both ends, bringing them together to form a closed circle[35,36]. Using a DNA ligase, the ends can be joined to have a truly circular molecule, which can be used as a template, with the original target serving as a primer to start the amplification. Using PLPs makes the reaction highly specific because hybridization with the target must be very accurate, especially at the ends of the PLP[37]. If this is not the case, the ligase will not be able to circularize the molecule and the amplification will halt at the break in the template.

Standard RCA is also most often performed using phi29 DNA polymerase. This is a DNA polymerase found in bacteriophage phi29, with excellent characteristics for isothermal amplification[38,39]. It works well between room temperature and 37 ˚C. This enzyme has great strand displacement ability, allowing it to unwind any dsDNA it encounters downstream of the amplification start, making it perfect for circular template amplification[38]. It also boasts high processivity[40], which means that once a molecule has bound to the template and initiated amplification, it will remain in the template for a long time. Phi29 DNA polymerase products usually reach around 70,000 nt in length before the polymerase detaches from the template[38]. Very importantly, this enzyme does not only polymerize DNA but also has a 3'-5' exonuclease domain[41]. This is used for proofreading, which entails removing newly incorporated but mismatched nucleotides and then continuing the polymerization. However, this exonuclease domain is capable of digesting any unmodified ssDNA oligos present in the reaction as well.

As previously mentioned, RCA generates long ssDNA products and the amplification is linear, meaning it copies the same template over and over. To generate the same products, but with exponential amplification, circle-to-circle amplification (C2CA) can be used[42]. C2CA is a method consisting of more than one round of ligation and RCA. After the first round of RCA, the products are monomerized into linear ssDNA copies of the PLP template using a restriction oligo (RO) and restriction enzyme. The RO is used to generate dsDNA in and around the cut sites for the restriction enzyme. Subsequently, the uncut RO serves as the target for the monomers to hybridize with. The monomers serve as PLPs and hybridize by bringing their ends together. Another RCA follows with a ligase creating a new circular template for each monomer of the original reaction, and a new amplification creating a long ssDNA product out of each circular template. This method provides for exponential amplification, although not a very efficient one, as the products become templates only a single time for every additional round of amplification. However, it yields significantly more DNA products than the linear RCA. While this process can be repeated more than one time, it is time-consuming and requires intermediate steps of enzyme inactivation and digestion, which

is why C2CA rarely involves more than two amplification reactions. A two-round C2CA improves sensitivity around a thousand-fold over RCA while generating the same type of ssDNA products.

In the works presented in this thesis, RCA and C2CA reactions have been carried out using different protocols and reagents. RCA was mainly used in Papers II, IV, and V, while C2CA was used in Papers I, III, and VI. Different enzymes and incubation times have been used, but the underlying principles of amplification remain the same: to generate long ssDNA for detection. The steps for both RCA and C2CA are displayed in Figure 4.

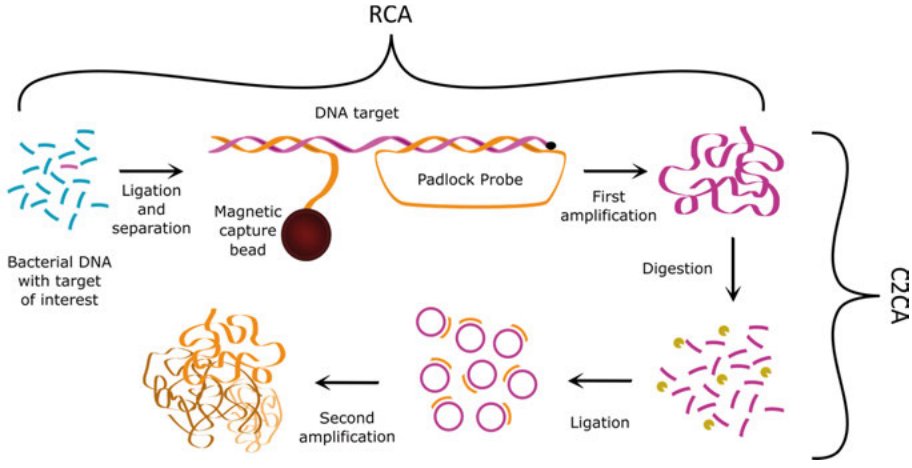

Figure 4: The basis of RCA and C2CA for biological samples as performed in this thesis. If isolation is not required, the magnetic capture bead is not necessary. RCA stops after the first amplification, while C2CA involves the further digestion of the products into a new template, and a second amplification, resulting in exponential amplification.

2.3.1. Padlock probes

As previously mentioned, PLPs are of high importance for RCA. However, not that much research has been done on PLP design. Before this thesis, PLPs used in other publications were long, about 100 nt, and focused on having strong binding to the target[43,44,45]. This approach is used in some of the Papers in this thesis such as Paper I, Paper II, and Paper IV.

However, the reason for this is unclear. Research on DNA circles has been conducted primarily in longer dsDNA circles. dsDNA circles are relevant for human health in bacterial plasmids, mitochondrial DNA, and viral DNA[46]. Extrachromosomal circular DNA, or eccDNA, has recently begun to be of interest as well[47]. However, all such DNAs are usually over 100 bp long, and knowledge of smaller circular sequences is scarce. The reason for this is that they are not stable. It has long been established that the length required for a stable, unconstrained circle of dsDNA in B-DNA shape is around 126 bp[48].

Padlock probes present an interesting problem. They start as ssDNA, which is known to behave as a flexible polymer, and in fact, it is known that circular molecules of as little as 11 nt can be amplified[49]. When PLPs hybridize with the target, they are partially dsDNA and ssDNA. But, once polymerization happens, the PLP becomes mostly dsDNA, as the complementary sequence is polymerized. When this happens, the dsDNA cannot stay in a stable B-DNA double helix shape. Studies show that a 42 bp circle must adopt a U-turn structures and deform[50], and it must be assumed that all circles of dsDNA under 126 bp must undergo at least some deformation from the B-DNA shape. This aids amplification, as phi29 and Bst polymerases show more efficiency in polymerization on templates with more constraint, and with half-turns in the double helix[51]. 126 bp yields a whole number when divided by the 10.5 length of a double helix turn of B-DNA. However, Joffroy *et al.* claim that template lengths resulting in half-turns of the double helix are better for amplification[51]. They hypothesize that this is related to the fraying probability of the last two nucleotides of the forming template. But this can also be explained by strand displacement. As the polymerase goes over the template after one round, it is fully dsDNA. Thus, it must unwind the downstream DNA to generate the ssDNA template for further polymerization. This is process is called strand displacement, and, the more tension on the DNA, the less energy required for it. Phi29 is known to stop polymerization less when the template is under more tension[52]. Thus, a shorter template, further away from the most efficient shape of a full double helix, increases the tension and allows the polymerase to work faster. Such findings are in line with reports that polymerases such as Klenow fragment, which have a much weaker strand displacement capability than phi29 and Bst, show the best performance in smaller circles of 34 nt[24]. It is likely that at such small sizes, the DNA might not be as stable as dsDNA, melting in certain regions to allow ssDNA to stabilize the shape of the molecule.

In this thesis, Papers III and VI deal with the optimization of the padlock probes based on the research described above.

2.3.2. Magnetic capture

A biological sample contains numerous molecules that are not of interest and may hinder the amplification reaction if they are present. Although RCA can be performed as previously described, magnetic capture of the DNA target of interest is used to isolate it from any other molecules that could potentially interfere with the amplification or detection process[53,54]. In this thesis, magnetic capture was consistently used for C2CA, regardless of whether the target was of a synthetic or biological nature.

For this, a magnetic microparticle (or capture bead, CB) is used. The CBs are functionalized with DNA oligos that bind the DNA target of interest outside of the PLP binding site. Using a simple permanent magnet, separation of

the CB-target complexes can be done easily. A thorough visual representation can be found in Figure 10, in Material and Methods.

3. Detection strategies

After the amplification process, the sample contains significantly more DNA compared to what it did originally. Still, it is not visible, so a setup for detection is required. The earliest technologies for this purpose originated in the 1970s, such as Southern blotting[55], and the 1980s, like restriction fragment length polymorphism (RFLP)[56]. It has become apparent that two main principles exist for detection. The first approach involves probe detection, in which a synthetic DNA oligo modified with a label can be washed over or incubated with the DNA of interest. If a complementary sequence is present, it will bind to it, and subsequently, detection becomes possible using the label, which can be radioactive, fluorescent, or another suitable marker. The second approach involves intercalating agents, which include molecules like ethidium bromide or more recent compounds such as Sybr Green. These molecules bind to DNA and emit fluorescence that can be detected. Nowadays, types of such chemicals that bind preferentially to dsDNA or ssDNA are commercially available. Note that while DNA probes only work if the complementary strand is present, intercalating agents bind DNA regardless of sequence. The idea behind intercalating agents and detection probes is visible in Figure 5.

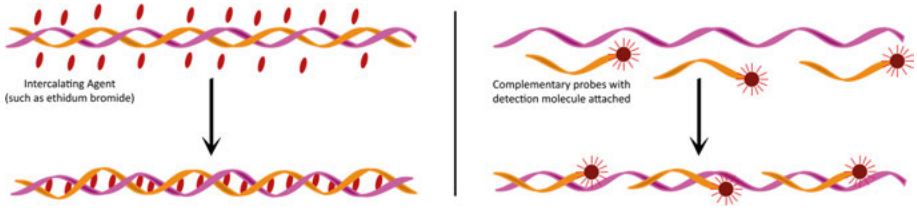

Figure 5: Main detection method principles. To the left, the use of intercalating agents such as ethidium bromide or Sybr Green. These molecules bind to the DNA and also deform the traditional helix shape. To the right, the use of detection probes. A complementary sequence oligo binds to the DNA. The probes are equipped with detection molecules such as biotins, fluorophores, nanoparticles, or other markers.

3.1. Gel electrophoresis

The most commonly used detection technique for DNA is electrophoresis in an agarose gel. This is a technique used to separate DNA according to their size. A gel made of agarose with ethidium bromide or another intercalating

agent is prepared [57], and DNA samples are loaded into wells at the upper end of the gel. Electrical current makes the negatively charged DNA molecules migrate through the gel in the direction of the positively charged electrode, which occurs at different speeds determined by the size and shape of the molecules, as well as the agarose content of the gel. Due to the fluorescent intercalating agent, the gel can afterward be imaged in an ultraviolet transilluminator to reveal the so-called bands at different heights, where the DNA of a similar size has accumulated. To determine the size of products, DNA ladders have been developed, and a pre-set mix of DNA of specific lengths is to be used as a reference. Gel electrophoresis is commonly used in combination with PCR[58], as the size of the amplification products is known. It is also frequently used in conjugation with LAMP and with other setups.

In this thesis, gel electrophoresis has mainly been used as a method to confirm results from other detection methods. This is because gel electrophoresis can detect total DNA, giving information on any unwanted amplification that might not be detected by sequence-specific probes.

3.2. Fluorescent tags

Although gel electrophoresis relies on fluorescence, several other methods employ similar principles. In these cases, fluorescent DNA probes are used, and detection is performed either in solution without the need for gel[59] or through fluorescence microscopy[60,61]. dsDNA dyes such as Sybr Green are widely used in PCR, especially in quantitative PCR (or qPCR). In qPCR, fluorescence images are captured during the amplification process [62], allowing real-time quantitative results.

Fluorescence spectroscopy is another commonly used method for DNA detection[63]. Modern spectrophotometers can perform fluorescence spectroscopy measurements on dozens or hundreds of samples quickly, using multiwell plates, which allows for high-throughput analysis.

Most fluorescent reagents, however, require careful handling, as exposure to light can quickly degrade them, potentially compromising the outcomes of numerous experiments and wasting costly compounds

Oligonucleotides coupled to a fluorescent molecule have been used in this work to determine the stability over time of the binding of biotinylated oligos to magnetic nanoparticles (MNPs) in Paper I.

3.3. Magnetic sensing

Several types of biosensors have been developed focusing on measuring magnetic properties. Biological samples are generally not magnetic, so magnetic particles or nanoparticles are used, usually with a probe to bind to the

biological element[64,65]. Such particles can be manufactured for this purpose with biocompatible coatings and molecules for attachment or capture of a surface or molecule, such as biotin or streptavidin[66,67].

Many magnetic sensors have been developed by taking advantage of properties of magnetic materials such as the Hall effect [68,69], giant magnetoresistance[70], or giant magnetoimpedance[71,72]. Measuring magnetic parameters in the sensor surface offers a baseline, which is disturbed by the binding of magnetic particles. This occurs only in the presence/absence of the DNA target of interest (or another analyte to be detected). These sensors are generally cheap and very sensitive, making magnetic biosensors an interesting option for the detection of biological molecules[73].

3.3.1 Brownian relaxation of MNPs and AC susceptometry

The dynamic magnetic response of suspended MNPs to an alternating magnetic field with angular frequency ω can be described by the complex magnetic susceptibility $\chi(\omega)$. The $\chi(\omega)$ for monodispersed, non-interacting MNPs is described by the Debye theory[74]

$$\chi(\omega) = \frac{m(\omega)}{H_{ac}} = \frac{\chi_0 - \chi_\infty}{1 + i\omega\tau} + \chi_\infty \quad (1)$$

with $m(\omega)$ being the complex magnetization, H_{ac} the amplitude of the AC magnetic field, χ_∞ being the high-frequency susceptibility and χ_0 the low field static susceptibility, and τ the relaxation time. The equation can be rearranged to

$$\chi(\omega) = \chi'(\omega) + i\chi''(\omega) \quad (2)$$

with the real and imaginary parts defined as

$$\chi'(\omega) = \frac{\chi_0 - \chi_\infty}{1 + (\omega\tau)^2} + \chi_\infty \quad (3)$$

and

$$\chi''(\omega) = \frac{(\chi_0 - \chi_\infty)\omega\tau}{1 + (\omega\tau)^2} \quad (4)$$

MNPs used in this work are superparamagnetic and exhibit Brownian relaxation behaviour[75], which depends on the rotation of a magnetic particle in a liquid. The Brownian relaxation time can be defined as

$$\tau_B = \frac{3\eta V_B}{kT} \quad (5)$$

With η being the dynamic viscosity of the liquid and V_B the hydrodynamic volume of the particle.

In AC susceptometry a time-varying sinusoidal AC magnetic field is applied to a sample by an excitation coil. The hydrodynamic volume of the MNPs increases when the probes on the MNP surface bind to a complementary molecule in the sample. This decreases the Brownian relaxation frequency of the MNPs, which define the frequency of the peak in the imaginary part of the susceptibility spectra described above This method was theoretically described at the turn of the millennium[76] and validated later on[77].

When performing RCA or C2CA, the products are incredibly large ssDNA molecules. The binding of these products shifts the nanoparticle's Brownian relaxation frequency to lower frequencies due to a sharp increase in hydrodynamic volume. This is the working principle behind the volume-amplified magnetic nanobead detection assay (VAM-NDA)[78], which was the foundation behind the work performed and reported in this thesis.

In this thesis, AC susceptometry measurements have been used as an accurate method to validate and quantify the results and to provide solid comparative data to optimize the methods. AC susceptometry was performed in a Dynomag (RISE Acreo, Göteborg, Sweden). The basic idea behind the Dynomag and the detection of hydrodynamic volume changes in VAM-NDA can be observed in Figure 6.

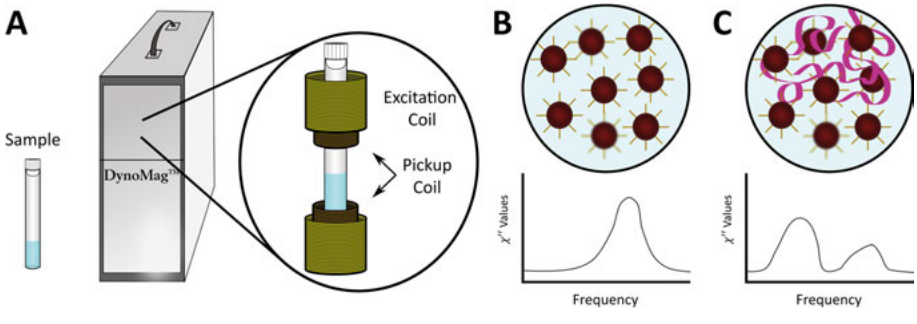

Figure 6: Basic setup and results obtained using the AC susceptometer Dynomag. **A:** sample tube shape, instrument, and inner workings. The sample is placed in the machine, where the excitation and pickup coils measure the magnetic susceptibility spectra. Part of the coils was removed in the illustration to see the pickup coil and sample. **B:** The imaginary part of the equation is plotted when the magnetic particles in the sample are unbound. **C:** as B, but when some of the particles are bound to an RCA product, the Brownian relaxation frequency becomes lower as the hydrodynamic radius of the bound particles increases. A smaller peak remains at a higher frequency, as not all particles are bound.

3.4. UV spectroscopy

UV spectroscopy is one of the most common ways to detect the quantity of DNA in samples. DNA absorbs light at around 260 nm wavelengths, facilitating its detection[79]. However, this method lacks specificity, providing

readouts only related to DNA concentration. Moreover, primers, dNTPs, and other reaction items can skew such readouts, making UV spectroscopy uncommon for the detection of amplification products unless a purification step is performed beforehand.

There are, however, alternative ways of using UV spectroscopy in DNA detection. These methods employ indirect detection, where a label is added to bind to DNA and alter the absorption wavelengths, or the use of nanoparticles that change absorption wavelengths when they aggregate, such as gold (Au) nanoparticles[80].

One of the main advantages of UV spectroscopy, similar to fluorescence spectroscopy, is the rapid analysis of hundreds of samples in multi-well plates.

In this thesis, UV spectroscopy and turbidity analysis have been used for the rapid analysis of numerous samples, greatly surpassing the speed of AC susceptometry. While not having the same accuracy as AC susceptometry, the use of multiple measurements per well showed considerable potential for comparative sample analysis.

3.5. Visual

Visual detection usually involves recognizing distinct differences between a sample where amplification has taken place and one where it has not, visible to the naked eye. However, it can also include other visual methods such as optical microscopy.

Visual detection is one of the most interesting detection methods for POC testing because it requires no or little readout equipment and no readout time. When working with microscopical molecules, obtaining results that can be visible to the naked eye can be challenging. However, different methods have been developed to overcome this. There are two main types of visual DNA detection, colorimetric and aggregation-based, and they are described below

3.5.1. Colorimetric

Colorimetric changes in a sample can occur in the presence of DNA that are so stark they can be seen by human eyes. There are two main colorimetric detection types of DNA amplified products, aggregation of nanoparticles with high surface-plasmon resonance (SPR) in the presence/absence of DNA, or solution changes due to the amplification reaction.

Aggregation of particles with a colour, such as Au nanoparticles, can result in a change of said colour. Solutions with Au nanoparticles in dispersed form have a red hue. If they aggregate, the solution changes to a purple or blue coloration. This is because spherical Au nanoparticles have a high SPR. SPR is a phenomenon that occurs when light hits a metal surface, and the light energy excites the surface electrons, resulting in an electromagnetic field[81].

This induces a strong absorption of the light, at a wavelength dependent on the size and shape of the particle[82]. This can be used to detect DNA specifically, by having the nanoparticles functionalized with probes to bind the DNA and aggregate[83], or unspecifically, by adding a salt. Positively charged salts will make the negatively charged nanoparticles aggregate by neutralizing the surface charge repelling them, unless DNA molecules of negative charge can stabilize the particles[84,85]. The basic idea of colorimetric change in Au nanoparticle solutions, when they aggregate, is displayed in Figure 7.

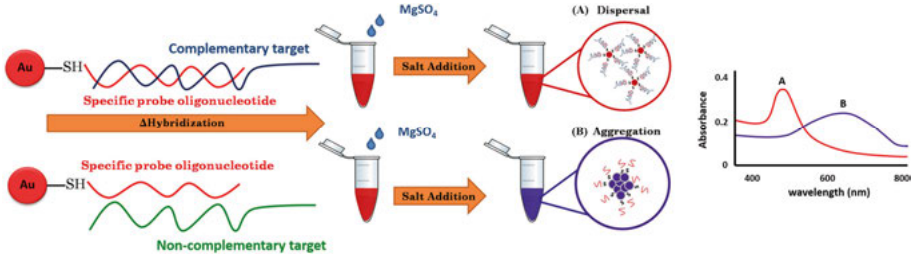

Figure 7: A schematic illustration of Au nanoparticle behaviour for the detection of DNA targets. Reproduced from Wachiralurpan *et al.*, 2018[86]

The process of DNA amplification also changes molecules within the reaction solution, by interaction with enzymes or amplification products. Such changes can be monitored, which makes this detection unspecific to the products generated, as only if amplification occurs is monitored, and not the product sequence. However, these methods offer the advantage of high sensitivity and fast, equipment-free detection. During the amplification, DNA polymerases use deoxynucleotides triphosphate (dNTPs), cleaving them into a deoxynucleotide monophosphate (dNMP) and a pyrophosphate (PPi). PPi accumulates as the amplification proceeds, and dyes that change colour in the presence of PPi can be used[87]. Enzymes that further cleave it into single inorganic phosphates (Pi) are called pyrophosphatases, and there are also dyes that change colour upon binding of the Pi. If both are added to the reaction mix, Pi dyes can be used for detection[88]. Due to the release of negatively charged ions, the pH of the solution can also change if it is not strongly buffered. This can lead to pH colour indicators used for colorimetry[89]. Lastly, DNA polymerases require metal ions, and the addition of Mg^{2+} or Mn^{2+} is required for their function. In LAMP, PPi precipitates with these cations, allowing the use of metal-binding dyes. During the reaction, the precipitation of the metals will revert the colour of the solution to the colour before metal ions were added[90,91].

Colorimetric readouts, using coloured polystyrene nanoparticles, in combination with image analysis, were used in Paper VI.

3.5.2. Aggregation

Although it has been mentioned before the use of Au nanoparticles in aggregation strategies, its outcome is primarily colorimetric. Aggregation of other types of particles and/or DNA itself can result in visual detection.

Aggregation strategies are mostly performed with RCA, due to its ability to produce long ssDNA products[38]. These products can spontaneously collapse into micrometer-sized aggregates [92]. Long ssDNA products can also be made to fold or aggregate in specific ways by altering and managing the template DNA of a PLP. A good example is the G-quadruplex formation in RCA products for fluorescence detection[93].

Nano and microparticles can selectively bind DNA through functionalization with complementary DNA oligos. Alternatively, they can bind DNA unspecifically through avidin or streptavidin interactions, or even through charge interactions, as DNA is negatively charged and positively charged particles may bind to it. Nonspecific aggregation of magnetic particles generating visual aggregates was described before, where micrometer-sized particles were aggregated using a permanent magnet, and resuspension was only possible if no RCA products were present in the solution[94]. In the research preceding this thesis, VAM-NDA has been known to generate distinct clusters and aggregates of DNA and oligonucleotide-functionalized MNPs. However, these clusters were only visible through different microscope techniques, such as transmission electron microscopy [95] or atomic force microscopy [96]

In this thesis, aggregation plays a central role, being a prominent feature in Papers II, III and VI. The thesis introduces and optimizes a novel detection method based on VAM-NDA, which is capable of producing visible aggregates between RCA products and nanoparticles.

3.6. Image analysis

Although image analysis is not inherently a standalone detection strategy, it is very often coupled with other strategies, usually of a visual or optical nature.

While a lot of details could be given for image analysis and its use in diagnostics, it mainly involves the development of software aimed at performing one or more of the following tasks: labelling, processing, and extracting data from images. This is crucial in high-throughput systems, where many images are acquired automatically, and manual processing would be very time-consuming. Artificial intelligence (AI) and deep learning have also emerged as valuable tools for extracting data and categorizing images, sometimes better than humans.

Image analysis has been used in various applications, such as obtaining data from gel electrophoresis images of DNA fragments[97], or analysing fluorescence in qPCR images and extracting relevant values[98]. In some cases, AI

can improve decision-making processes, such as optimizing the DNA yield for sequencing from tumour tissue[99]. One of the biggest platforms for image analysis in the biological sciences is ImageJ[100,101], an open-source program using Java. ImageJ is capable of the simplest analysis and processing of images while featuring many open-source plugins and the chance to implement macros to run on any set of images.

Image analysis was used in Paper VI for analysing samples in multiple target detection based on coloured nanoparticle aggregation.

4. VAM-NDA

VAM-NDA, published for the first time in 2008, relies on detecting changes in the rotation of MNPs. These MNPs, exhibiting Brownian relaxation behaviour, are functionalized with oligos complimentary to DNA amplification products, which results in the binding of the MNPs and DNA[78]. DNA amplification is usually based on techniques like RCA or C2CA, which produce remarkably large products[102]. The MNPs are added after the DNA amplification and bind to the DNA products. The binding process depends on factors such as the oligo sequence and complementarity to the products, oligo surface coverage, and particle size, resulting in the formation of different types of clusters or aggregates[96,103]. Upon the MNPs binding, the hydrodynamic volume of the particles increases, leading to a change in their Brownian relaxation. These dynamic changes, detailed in section 3.3.1, are measured using a magnetometer.

A superconducting quantum interference device magnetometer was originally used for such purpose[78], although later on a faster and cheaper commercial AC susceptometer was used[104] and an optomagnetic readout device has been tested as well[105]. Free and unbound MNPs exhibit a peak in the imaginary part of the frequency-dependent magnetization spectra (χ''), which value is directly proportional to the total quantity of magnetic material in the sample. The frequency at which this peak is depends on the size of the MNPs. The binding of these MNPs to the large DNA products shifts the frequency peak to lower frequencies and reduces the values of the frequency peak representing the unbound MNPs. This allows for comparative analysis of samples by comparing the values of the peaks in negative control (NC) samples with other samples[78]. A visual representation of how VAM-NDA works using RCA and how the reaction differs between positive and negative samples can be found in Figure 8.

VAM-NDA has successfully been used to detect resistance genes in *Mycobacterium tuberculosis*[106], detection of two sequences in one sample [105], and detection of DNA in a homogeneous assay combined with a microfluidic setup [107].

However, the basis of VAM-NDA leaves room for improvement, as there are unknowns regarding the RCA products and the binding behaviour of the MNPs. As the RCA products grow, they become so large that they collapse into micrometre-sized coils[92]. This begs the question of if and how the MNPs

bind effectively. Long ssDNA strands behave like negatively charged random polymers, and their collapse might occlude potential binding sites. A technique used to increase the sensitivity of VAM-NDA was real-time sensing[108], which has more potential, due to the possible binding of the products before their collapse, and stabilization of the ssDNA by having dsDNA regions where the probes might bind.

But the question of whether the MNPs are binding as efficiently as possible and how the DNA coils behave remains. Most end-point sensing protocols required a relatively long step for binding, of 20 minutes at 55 ˚C, before measurement in the AC susceptometer[104].

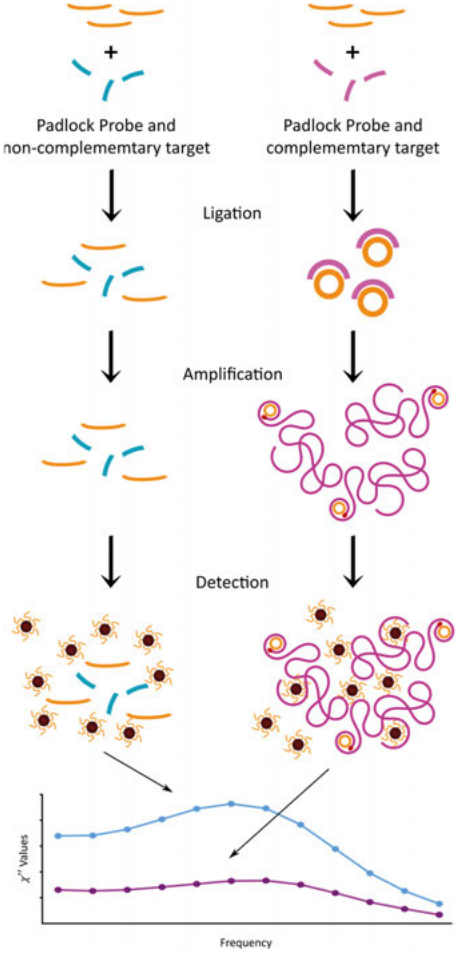

Figure 8: The principle behind VAM-NDA. Hybridization and circularization of the padlock probe only happen if the target with the complementary sequence is present. If so, amplification and binding of particles to the products occur, resulting in low χ'' values. If hybridization and ligation do not occur, there is no template for amplification, and the particles cannot bind any products, as they are not present. This results in high χ'' values due to the free, unbound magnetic particles.

5. Materials and Methods

This section aims to explain the reasoning behind some of the protocols and materials used in this thesis from an overarching perspective that cannot be found in the individual publications. For full protocols, please refer to the individual papers.

5.1. Synthetic oligonucleotide design and use

Synthetic oligonucleotides are used in all publications in this thesis, as they are required for recognition, amplification, and detection. The design of these has been performed and optimized depending on the desired functions. Below is a description of the main types of oligonucleotides used and their sections of relevance for their function.

5.1.1. Design and use of padlock probes

Padlock probes are used in all papers presented in this thesis, with part of Papers III and VI focusing on the optimization of padlock probes.

PLPs are linear sequences that serve the purpose of recognizing a DNA target and hybridizing with it, bringing the 3' and 5' ends of the PLP together for subsequent ligation. The importance of their design is evident, as seen in some of the works within this thesis. The most straightforward approach for designing a PLP involves identifying the essential regions required for its proper functionality and the subsequent amplification products it produces. In this work, the regions of interest include the target recognition sequence, the restriction segment, and the detection oligonucleotide (DO) binding site. Target recognition involves binding to the DNA target, the restriction segment consists of a sequence in the amplification product that can be cleaved by a restriction enzyme, and the DO binding site encompasses a sequence in the product that can be bound by probes for detection.

The temperature for ligation, amplification, digestion, and binding of the products by the DOs will dictate the length of each region, as melting temperature is determined by the sequence and length of the corresponding regions.

In this thesis, the arms (the two sides of the PLP that compose the target recognition sequence) of the PLPs have typically been around 15 nt each, the

restriction segment around 20 nt, and the oligo binding site within the range of 20-30 nt. In Paper VI, the length of the PLPs was reduced to 60 nt, which necessitated merging the target recognition sequence and the oligo-binding site. This was necessary since shortening the probe while keeping both regions separate and of similar length was not possible.

In the context of antibiotic resistance, several genes may provide resistance against the same antibiotic. Through effective PLP design, it is possible to employ several PLPs in a single reaction, each with a different target recognition sequence but having the same oligo-binding site. This can allow the detection of resistance against a specific antibiotic, regardless of which of several genes providing the resistance may be present. However, if the target recognition and oligo binding site are merged, achieving this with a single DO is no longer viable. Nevertheless, it is feasible to use several types of DOs with different sequences for the functionalization of nanoparticles used in the detection.

The design and size-related changes in the padlock probes within this thesis, as well as the different sites, can be found in Figure 9. This scheme also provides the basic structure of the ROs and DOs

5.1.2. Restriction oligonucleotides

ROs bind to the RCA products, generating dsDNA in and around a sequence recognized by a restriction endonuclease. This binding allows digestion and monomerization of the RCA products. In this work, the restriction enzyme AluI was used for monomerization, and thus all ROs shared the same restriction sequence of 5'-AGCT-3'. The same RO was used for the majority of products, as nearly all PLPs had the same restriction segment sequence. Additionally, the undigested ROs also serve as targets during the ligation and amplification of the second round of RCA in C2CA.

5.1.3. Detection oligonucleotides

DOs are used for the detection of the amplification products. The DOs used in this thesis are equipped with a biotin group at one end, usually located at the 5' end, along with a 20-30 nt sequence, the binding site, that is complementary to the amplification products.

The biotin and the binding site are separated by a T-tail, usually consisting of 20 T nucleotides. This T-tail separates the nanoparticle from the amplification product, reducing any potential steric hindrance, especially since the nanoparticles are considerably larger than the nucleotide sequence.

Nanoparticles were functionalized with DOs by incubation in solution together for at least 10 minutes at room temperature, where the streptavidin molecules on the particle´s surface bound the biotin residues in the DOs.

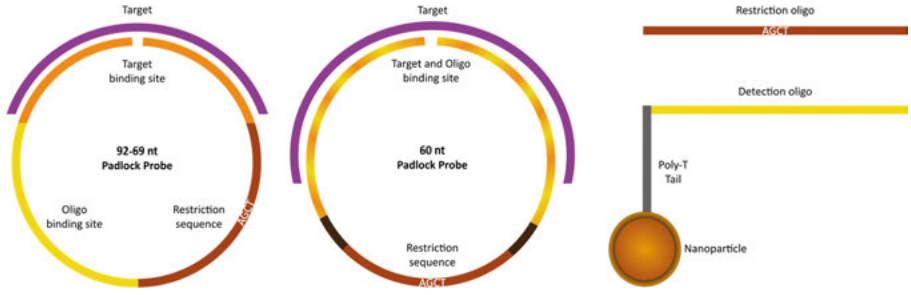

Figure 9: Design and outlook of the sequences designed in this work. To the left, it showcases the design of longer PLPs (92-69 nt), highlighting their distinct regions. The shorter PLPs (60 nt) are displayed in the middle, where the target binding site and oligo binding site are merged. Note that the target binding site is not necessarily longer in the 60 nt PLP; it just occupies a higher percentage of the sequence. To the right, the restriction and DOs are presented. Their colours correspond to sequences within the PLP, as these oligos bind to the products generated by RCA, which are complementary to the PLP. Thus, the restriction sequence regions of the PLP and the RO have the same sequence, and the same occurs for the oligo binding site and DO for RCA.

5.1.4. Capture oligonucleotides

Capture oligos (COs) are used to capture and isolate the target of interest using magnetic particles. They have a biotin group at either the 3' or 5' end, allowing binding to the streptavidin-coated T1 Dynabeads magnetic microparticles, also referred to as capture beads. The opposite end of the COs hybridizes with the sequence of interest. A 20 nt T-tail is also included to separate the biotin from the recognition sequence, as with the DOs. Magnetic separation allows the isolation of the capture beads-CO-target-PLP from any remaining unhybridized sequences, biological DNA fragments, or molecules. The basic structure and crucial function of the CO and magnetic separation are shown visually in Figure 10.

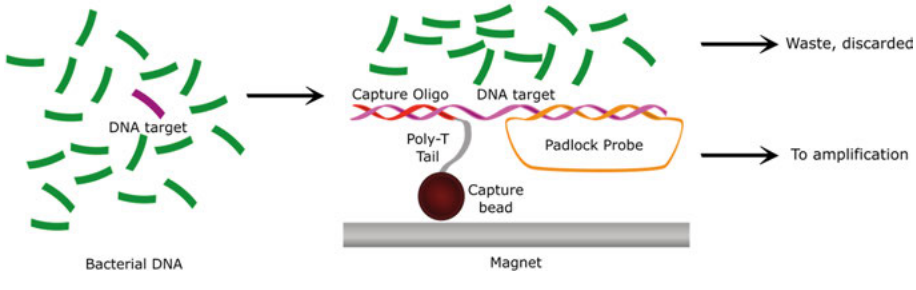

Figure 10: Magnetic separation of a DNA target from a larger DNA pool. The CO hybridizes with the DNA target at one end and binds to a capture bead through a biotin at the other end. Using a magnet, the complex containing the target DNA can be isolated from the remaining DNA, which is then discarded. The DNA of interest proceeds to the amplification step.

5.2. RCA and C2CA

In this thesis, RCA and C2CA were performed using different enzymes, incubation times, and temperatures. Presented below is a brief overview of the selected enzymes and the reasoning behind their choice, along with the specific incubation times for each step.

5.2.1. DNA Ligases

DNA ligases are used to join both ends of the PLPs upon target recognition, and this is required for amplification. If ligation does not occur, no circular template can be amplified.

For RCA using synthetic targets in stock solutions, ligation was done with T4 DNA Ligase. This ligase was used at 37 ˚C, typically for 15 minutes of ligation. T4 DNA Ligase requires adenosine triphosphate (ATP) and performs effectively in Thermofisher´s phi29 DNA polymerase buffer when supplemented with ATP. This made it a suitable candidate for the second round of ligation during C2CA, as the ligase is added with the polymerase, and both work in the phi29 polymerase buffer.

When conducting RCA with biological or synthetic targets in combination with capture beads and CO, either Tth DNA ligase or Ampligase was used. These enzymes share the same buffer and exhibit similar performance, both capable of ligating DNA at higher temperatures. This is preferred in biological samples, as the increase in temperature reduces the unspecific binding of the PLPs to other DNA fragments, increasing ligation specificity. With these enzymes, ligation occurred faster, typically ranging from 5-10 minutes, and at higher temperatures, such as 55 or 60 ˚C. The buffer used in this case differs from phi29´s buffer. Therefore, a magnetic separation step was employed to transfer the ligated products to the phi29´s buffer for the subsequent RCA reaction. To ensure that all target molecules effectively were bound, an excess of PLPs was used.

Both Ampligase and Tth ligase are nicotinamide adenine dinucleotide-dependant, and do not require ATP.

5.2.2. DNA Polymerases

Phi29 DNA polymerase was used in all the Papers in this thesis. However, as explained in Paper V, different manufacturers of phi29 were tested, and their buffers differed, as did the quantity of products generated from the same initial DNA amount, using the same quantity of polymerase units. Thermofisher´s phi29 DNA polymerase exhibited optimal performance at 37 ˚C, and this manufacturer´s enzyme was used in all Papers in this thesis.

Furthermore, phi29 DNA polymerase mutants, equiphi29 (Thermofisher), and phi29-XT (New England Biolabs) were also tested. Both can amplify

DNA at higher temperatures, although most of their details and buffer composition are proprietary. For a detailed comparison between phi29 and phi29-XT, refer to Paper VI.

Phi29 DNA polymerase and its mutants have an exonuclease domain that works in the 3' to 5' direction. This feature provides proofreading and high processivity, but it can be a limitation in certain applications involving ssDNA. As Paper V shows, ssDNA is quickly digested by phi29 unless present in high quantities or modified to avoid digestion.

In Paper V, Bst 3.0 DNA polymerase was used, primarily because it lacks an exonuclease domain. Reactions with this polymerase are usually carried out at higher temperatures, approximately around 60 ˚C.

5.2.3. Restriction endonucleases

Restriction endonucleases or enzymes were used for two reasons: firstly, for digesting RCA products into monomers as part of the C2CA process, and secondly, for digesting the biological DNA target to generate targets of suitable length.

For the monomerization, AluI was used, with an incubation of 2 to 5 minutes, as the enzyme was added in excess for quick digestion. However, in Paper VI, when phi29-XT was used, monomerization involved two incubations, one at room temperature and another at 42 ˚C. For all other works, a 3-minute incubation at 37 ˚C was used.

For the digestion of DNA from biological samples in Paper III, plasmid DNA in a stock solution was digested for 1 h. AluI and BsuRI were used in Thermofisher´s Tango buffer. Thermofisher specifies AluI to have 100% efficiency in said buffer, while BsuRI has 50%. For this reason, the quantity of BsuRI added to reactions containing Tango buffer was twice the quantity of AluI.

5.3. Micro- and nanoparticles

Particles were used for both magnetic separation and the detection of amplification products. Below is a description of the particles used and the methods of functionalization strategies used. All the particles used in this thesis are commercially available. A portrayal of cross-sections of all the particles used can be found in Figure 11.

5.3.1. Dynabeads

Dynabeads MyOne Streptavidin T1 (Invitrogen) were used as capture beads in this thesis. These Dynabeads are 1 µm superparamagnetic monodisperse particles with a monolayer of streptavidin to allow the binding of any

biotinylated surface or molecule. The iron content is made up of ferrites. They are designed for nucleic acid isolation.

Dynabeads were added after ligation to bind COs present in the ligation mix.

5.3.2. BNF nanoparticles

The MNPs used for detection in this work were nanoparticles of bionized nanoferrite (BNF) with a diameter of 100 nm. These nanoparticles consisted of a core-shell composition, with the core comprising 75-80% (w/w) of BNF and a shell of hydroxyethyl starch with covalently bound streptavidin on the surface. These are commercially available from Micromod Partikeltechnologie (product code 10-19-102).

Functionalization of the nanoparticles was carried out after three washes with a washing buffer using a permanent magnet and the number of oligos per particle differed from one paper to another. For more information regarding oligo coverage, refer to Paper I.

5.3.3. Coloured polystyrene nanoparticles

Polystyrene nanoparticles (PS-NPs), with a diameter of 200 nm, dyed polymer in Crimson Red and Cabo Blue colours, and coated with streptavidin, were purchased from Bangs Laboratories Inc. (Fishers, Indiana, USA) (product codes CDCB001 and CDCR001) These nanoparticles were used for detection in Paper VI.

The PS-NPs were functionalized with around 1500 oligos per particle. Despite this high ratio, only a fraction of streptavidin sites was bound by oligos. To decrease any potential unspecific binding due to free streptavidin, an excess of biotin was added after a short incubation step in the presence of the oligos, blocking any remaining free streptavidin residues.

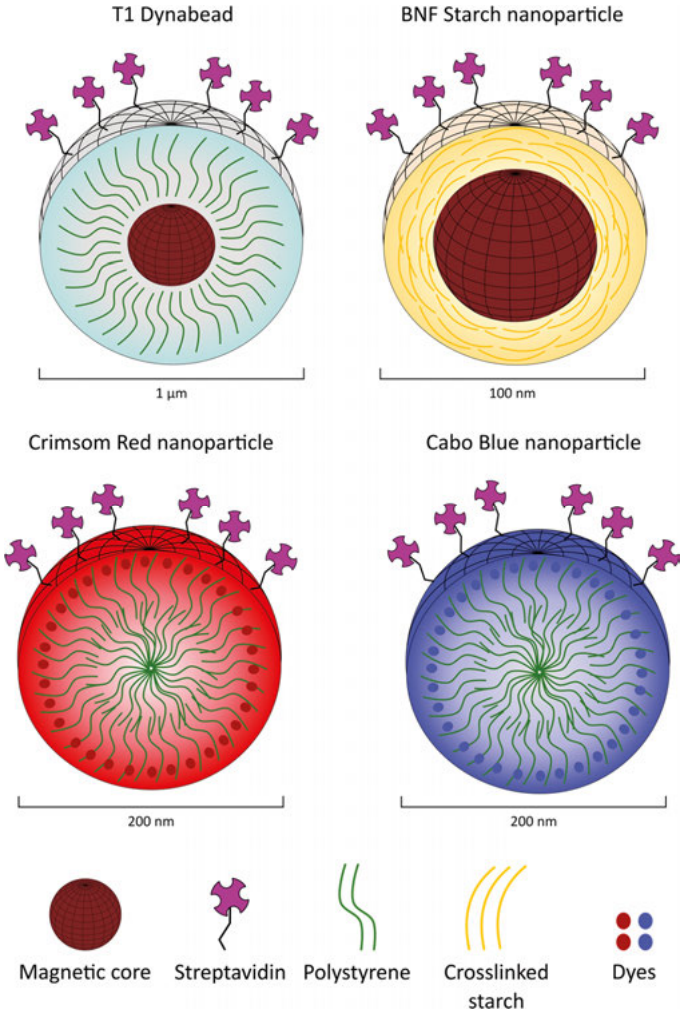

Figure 11: Cross-sections of the different nanoparticles used in this work with a schematic representation of the content of the different layers and surface functionalization. Note that, in solution, particles with a magnetic core always are visually brown.

5.4. Detection of amplification products

Below is a short reasoning behind the specific setup and function of the detection techniques used in this work

5.4.1. UV spectroscopy

UV spectroscopy was used to determine the turbidity of DNA samples in clear polystyrene 96-well plates with flat bottoms after the aggregation with MNPs. The idea behind this type of detection method was that in samples where

aggregates formed, the sample became clearer, allowing more light through. While the presence of the aggregates may be visible to the naked eye, DNA quantification was harder to do visually. In this regard, UV spectroscopy showed less accuracy compared to AC susceptometry, as the latter measures the binding of MNPs, while UV spectroscopy focuses on the number of nanoparticles remaining in suspension. It is important to note that nanoparticles can bind to DNA and remain suspended in the solution. However, using a UV spectrometer significantly reduced the time required for analysis compared to AC susceptometry, and allowed for comparative analysis of samples.

The presence of aggregates was an issue, as they have a very dark coloration. If measurements were done in the vicinity of an aggregate, the aggregate was likely to affect the results. Although other approaches, such as removing the aggregate, were tested, the most effective solution was to perform multiple measurements per well. A total of 12 measurements were taken in a circular, filled, shape, positioned 1,500 nm away from the well edge to avoid potential optical interference from the well's edge.

Measurements were feasible at any wavelength, yet lower wavelengths consistently yielded higher values, making discrimination between samples easier. For this reason, 350 nm was chosen as a low wavelength where the presence of DNA did not interfere with the measurements.

5.4.2. AC susceptometry in the Dynomag

AC susceptometry has been performed the same way in all the Papers in this thesis with liquid samples having a volume of 200 µL. The samples were pipetted into the vials and their volume was adjusted to 200 µL, regardless of their original volume.

While the specifics of the measurement setup have changed across the papers, the objective has remained the same: recording the χ''_{max}. The relaxation frequency for the unbound BNF MNPs used throughout the thesis was centred around 100 Hz, usually within the range of 75-125 Hz. Although the number of points has differed across the different papers, this frequency range was always included.

5.4.3. Gel electrophoresis

The main reason for employing electrophoresis was to validate results obtained through other techniques. Gel electrophoresis provides unspecific DNA detection, while the use of DOs ensures the detection of only complementary sequences.

Gel electrophoresis was used sparingly due to its low detection limit in comparison to AC susceptometry, UV spectroscopy, or visual aggregation detection. When gel electrophoresis was performed, a larger quantity of DNA

target was needed to generate enough amplification products for detection with this technique.

Moreover, the size of RCA products is too large for pores in the agarose gel, causing them to accumulate at the top of the lanes, with minimal movement into the gel. Thus, very little information regarding RCA product size can be found with gel electrophoresis.

For all these reasons, gel electrophoresis was mainly used to determine if there was an increase or decrease in total DNA products in different situations and conditions throughout the works of this thesis.

5.4.4. Limit of detection

Across the different papers, the limit of detection (LOD) has been consistently calculated using the same approach. These LOD values were employed in the analysis of AC susceptometry and UV spectroscopy results. The LOD is defined as a threshold value, determined by calculating the mean of three NC sample read-out values minus three times the standard deviation (SD) of the NCs.

If the average read-out value plus the SD of a positive sample is below this limit, it is considered detectable.

Additionally, it is worth noting that LOD has also been described as the minimum quantity of target DNA in a sample that is still considered detectable, whether through instrument readouts or visually.

5.4.5. Image analysis

Image analysis was used in Paper VI to demonstrate, as a proof of concept, that simple phone images could be used for end-point detection of samples after multiplexed detection with coloured PS-NPs. The images were acquired with a common smartphone, placing the tubes on a white sheet of paper, and using a manual white balance to acquire all images with the same hue of white.

ImageJ was used for image analysis, and the images were split into three using the “lab stack” option in the software. This allowed each image to show the values for each pixel in CIELAB space, a 3D space representing a lightness gradient (L), a red-to-green gradient (A), and a yellow-to-blue gradient (B). The values go from positive (white) to negative (black). Thus, red and yellow colours will provide positive values in the A and B channels respectively, and be represented by white, and green and blue, with negative values, represented by black. A visual representation of CIELAB space and images of some negative samples converted into a lab stack can be seen in Figure 12.

Measurements were done using ImageJ of the values of single pixels in the solution of the samples to determine the quantity of the different particles in the solution.

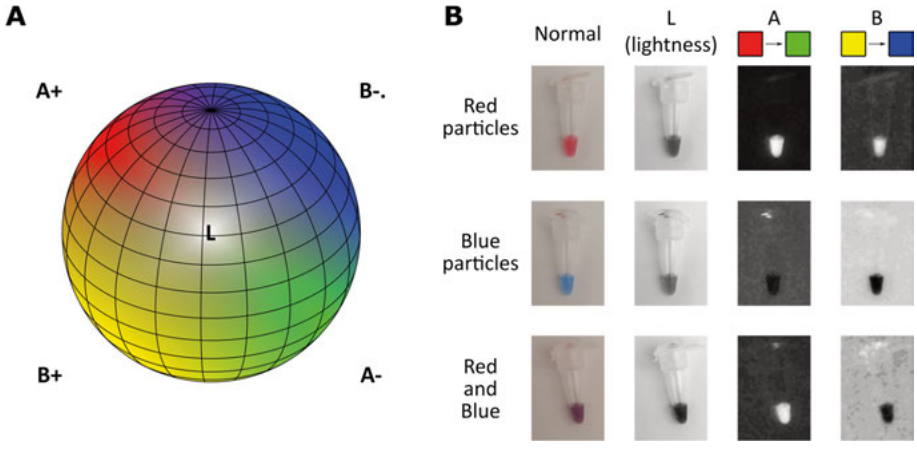

Figure 12: CIELAB space and images split by the Lab stack function in Image J. **A:** a visual representation of CIELAB space, a 3D space with the axis L, A, and B. **B:** NC samples containing only coloured nanoparticles imaged with a phone camera and split into L, A and B channels. Reproduced with permission from Paper VI.

6. Results

In this section, the overall advances from all the Papers in this thesis can be found. For specifics, refer to each Paper individually. The majority of the work is centred around three different yet related topics. First is the optimization of the bioassay, which concerns methodological and procedural advances to improve the performance of different aspects within the assay. Second, the discovery of an inhibition of phi29 by ssDNA oligos. Third, the development of a novel detection method employing nanoparticle aggregation instead of magnetic susceptibility sensing to detect the presence of amplified DNA.

6.1. Optimization of the bioassay

6.1.1. Padlock probe size

When it comes to RCA, PLPs are crucial to recognize the target and serve as a template. Previous research indicates that the length and shape of PLPs determine the efficiency of amplification, as it affects the speed of polymerization of the template[51,52]. Furthermore, reducing the PLP size results in more repeats and binding sites in a product of equal length. Lastly, the PLP size plays a crucial role in C2CA, as each monomer from the first amplification serves as a new template for the second amplification. Thus, shorter PLPs mean more targets for the second amplification.

For these reasons, in Paper III, a padlock probe against *Vibrio cholerae,* initially of 92 nt, was shortened to 69 nt. This smaller PLP retained all the required sequences needed for its function, while also falling within the parameters for best amplification bias according to Joffroy *et al*[51]. The detection of C2CA products using the 92 and 69 nt PLPs can be seen in Figure 13A, showing better detection using shorter PLPs. Moreover, reducing the amplification times by 25% for the shorter probe (equivalent to the length reduction of the PLP, from 92 to 69 nt) still provided better results than full-time amplification using the long probe. This suggests that the changes in the probe extend beyond monomer size changes, indicating a higher amplification efficiency achieved by reducing the length of the PLP.

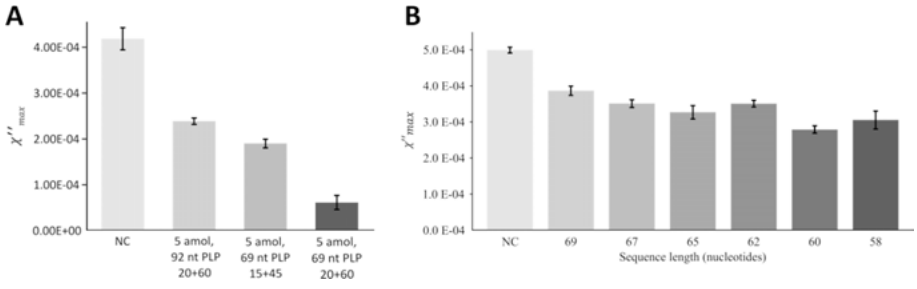

Figure 13: Effect of the size of padlock probe in C2CA. The graphs show AC susceptometry results comparing different PLP sizes. **A:** 69 vs 92 nt PLP using C2CA. The last numbers for each sample indicate the time for the first and second amplification reactions, in minutes. **B:** Comparison of different PLP sizes, from 69 to 58 nt. Error bars represent SD. N=3. Modified with permission from Paper III and Paper VI.

Later, in Paper VI, the PLP size was further shortened to 60 nt. Since Joffroy *et al.* did not test probes smaller than 67 nt[51], an analysis of different lengths was done, revealing improved results using a 60 nt PLP, as shown in Figure 13B. While shorter probes could be a possibility, fitting the required regions for function within less than 60 nt might pose a design problem. However, future investigations should explore the effects of further reducing the size of the PLPs.

6.1.2. Magnetic capture

The need for magnetic capture arises from the issues that proteins and other molecules might pose to the amplification reaction, as well as the much larger quantity of non-target DNA in biological samples compared to target DNA.

Moreover, it allows the transfer of the DNA target-PLP from the ligation to the amplification step, allowing for a different buffer to be added, and removing unreacted PLPs that would hinder the amplification. Different aspects of magnetic capture have been investigated in different papers.

In Paper I, it is demonstrated that magnetic capture works efficiently to isolate the target of choice from a large pool of DNA. A comparison between samples with only the target to be amplified and samples spiked with 100 attomoles of a large 220 kb digested plasmid can be seen in Figure 14. There was only a slight loss of sensitivity. While this seems to point out at a slight loss of target, there seems to be no unspecific amplification from the large quantity of DNA added, showing the ability of magnetic capture to effectively isolate the target of interest.

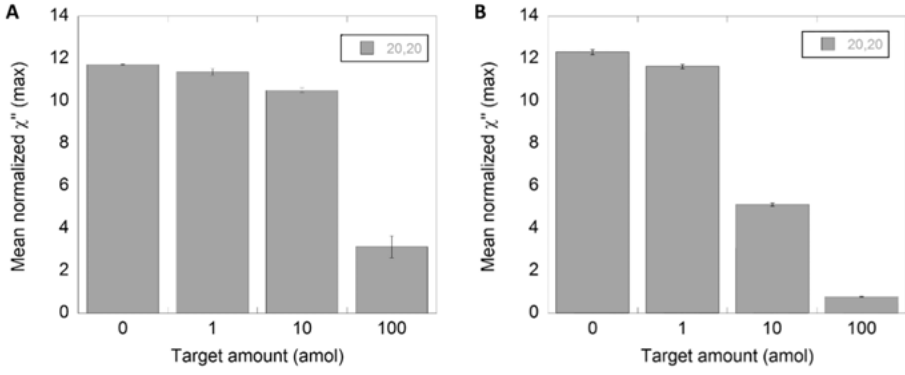

Figure 14: Efficiency of magnetic capture. AC susceptometry results from C2CA performed with different quantities of a synthetic target. **A:** Samples spiked with 100 attomoles of plasmid pUUH239.1. **B:** Samples containing only the synthetic target. Error bars represent SD. N=3. Modified with permission from Paper I.

In Paper IV, Dynabeads, serving as magnetic capture beads, are also used to increase the hydrodynamic size of the RCA products. This aims at improving readouts by enabling shorter amplification times. The addition of 1 µm Dynabeads, attached to the amplification products, influences not only the hydrodynamic volume of the MNPs through amplification products but also through the presence of Dynabeads. This strategy reduces RCA time without losing sensitivity, as can be seen in Figure 15. A comparison of different RCA times shows minimal variation when the RCA time is increased above 20 minutes.

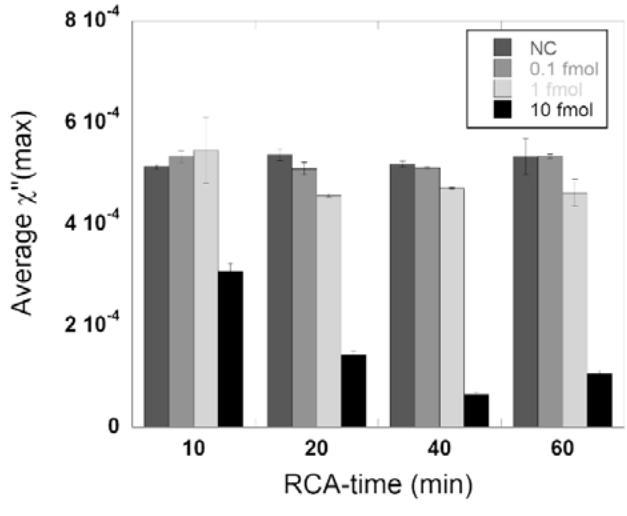

Figure 15: RCA on a bead. Results of different RCA amplification times when the target is coupled to a 1 µm magnetic capture bead. The increase in time does not improve the sensitivity after 20 minutes of RCA time. Reproduced with permission from Paper IV.

6.1.3. Amplification

Several investigations have been conducted to improve RCA, with a focus on product generation and amplification time, to improve the overall detection.

In Papers I and III, the comparison between RCA and C2CA shows a minimum 400x improvement in the LOD due to the second amplification. This improvement is shown in both AC susceptometry results and visual aggregation detection. With the first amplification in C2CA being around 20 minutes, this is a great improvement in sensitivity time-wise. Figure 16 illustrates the comparison between the LOD for RCA (reported in Paper II) and the LOD for C2CA (reported in Paper III).

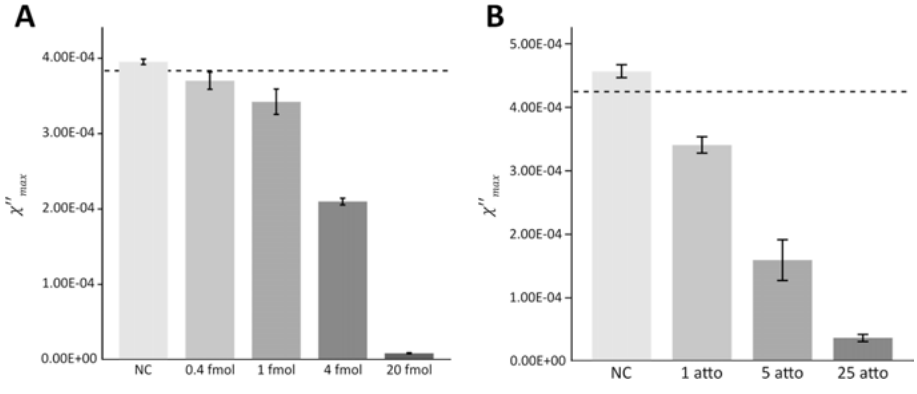

Figure 16: Sensitivity for RCA and C2CA. AC susceptometry results for **A:** RCA, taken from Paper II. **B:** C2CA, taken from Paper III: Dotted lines represent the LOD. Error bars represent SD. N=3. Modified with permission.

The amplification times for both RCA and C2CA were investigated in Papers I, IV, and VI. Initially, RCA was conducted for 60 minutes, as was the second step of C2CA. The duration of RCA amplification and the second step in C2CA are related to the size of the product. Larger products, up to a certain extent, provide higher sensitivity due to the increased hydrodynamic size of the DNA products, and enhanced aggregation of the DNA molecules. However, in Paper I, it was found that even 20 minutes for each C2CA amplification step was sufficient for detecting 1 attomole of a synthetic target. In Paper IV, 20 minutes of RCA provided similar results to longer amplification times, due to the hydrodynamic size of the products being boosted by the bound Dynabeads. However, 10 minutes showed much worse performance, as presented in Figure 15, leading to a general avoidance of RCA times shorter than 20 minutes.

After optimizing the padlock probe design, leading to an improved amplification, it was theorized that RCA time could be decreased while still producing visible aggregates of MNPs and amplification products. In C2CA, the most sensitive results were obtained when both amplification steps were set

for 40 minutes, maximizing the number of monomers for the second reaction while keeping the final products at an ideal length for effective aggregation.

6.1.3.1. Enzymes for amplification

Phi29 DNA polymerase from Thermofisher (Waltham, MA, USA) has been the enzyme used in the majority of the amplification reactions throughout this thesis. This choice is attributed to phi29's great strand displacement ability and high processivity[38,40]. That is why phi29 has become a staple for RCA worldwide. In Paper V, different phi29 DNA polymerase manufacturers were investigated, as can be seen in Figure 17A, finding Thermofisher's as the best-performing for RCA. This is likely caused, at least in part, by the buffer, as the enzyme remains the same across the different manufacturers. The buffers from Lucigen (Middleton, WI, USA) and NEB (Ipswich, MA, USA), share the same composition, which differs from that of Thermofisher's. The difference in performance between Lucigen's and NEB's phi29 was surprising and unexplained as of yet.

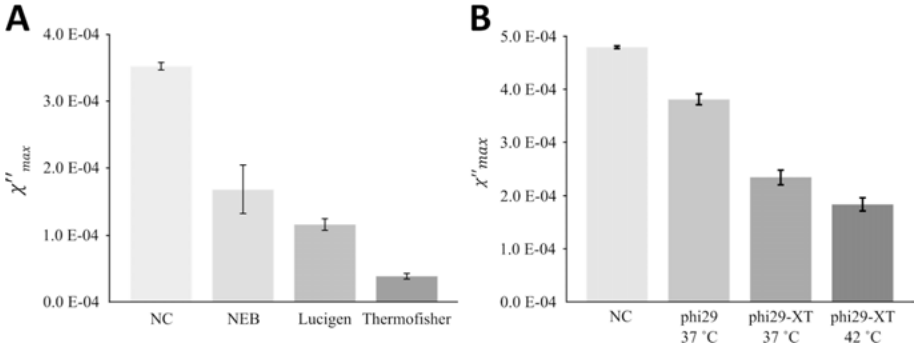

Figure 17: Efficiency of different phi29 polymerases and buffers. **A:** different performances of phi29 DNA polymerases from different manufacturers in their respective buffers in RCA reactions at 37 ˚C. **B:** C2CA results of phi29 DNA polymerase and phi29-XT at different temperatures, in Thermofisher´s 1x phi29 buffer. Error bars represent SD. N=3. Modified with permission from Papers V and VI.

In Paper VI, phi29-XT, a mutant introduced recently to the market by NEB at the time, was tested with great success, as shown in Figure 17B. Phi29-XT showed great activity in the Thermofisher´s phi29 DNA polymerase buffer, which had been previously used to optimize all the reactions in C2CA where multiple enzymes were used (digestion, second ligation and amplification).

6.1.4. Detection using MNPs

When it comes to the detection of amplification products, there are important issues regarding the MNPs used for binding that had to be evaluated.

In Paper I, the functionalization of the MNPs was examined through the binding of fluorescent oligos to the particle surface. The results can be seen in Figure 18. On average, MNPs demonstrated the capability to bind at least 100 oligos per MNP. Moreover, the oligos show low detachment for up to six months when the functionalized MNPs are stored in PBS. This is highly relevant for ease of use in clinical settings, where solutions of functionalized MNPs can be prepared ahead of time.

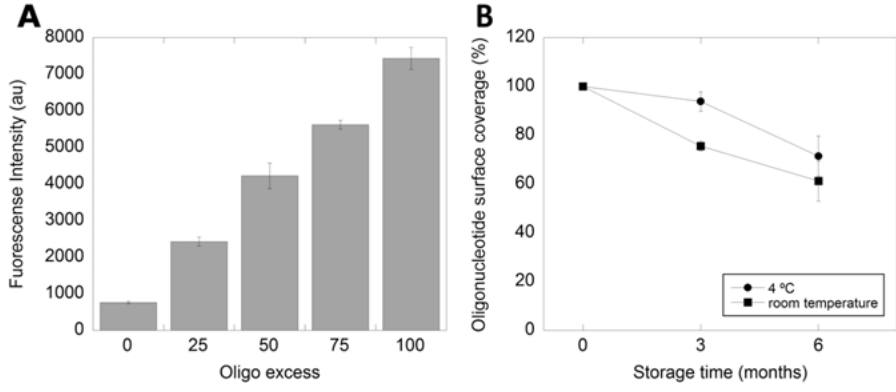

Figure 18: Functionalization of MNPs and stability of binding over time. **A:** Fluorescence intensity of MNPs functionalized with different quantities of fluorescent oligos, after washing. **B:** Coverage of oligos after functionalization, or storage for 3 or 6 months. Error bars represent SD. N=3 Reproduced with permission from Paper I.

Effective binding of the MNPs to the amplification products is crucial for detection. When using AC susceptometry, detection is done on the binding of MNPs and not the quantity of DNA directly. In Paper III, an experiment was performed using two DOs capable of binding two different sequences within a single repeat, as it could improve detection by doubling the potential binding sites. Although different approaches were used in the attempt, such as having two pools of MNPs with different DOs or using a single pool of MNPs functionalized with both types of DO, no significant improvement in detection could be seen. The results are shown in Figure 19, and the cause for the lack of improvement may be attributed to steric hindrance caused by MNPs in close proximity, preventing more binding in regions of the RCP too close together.

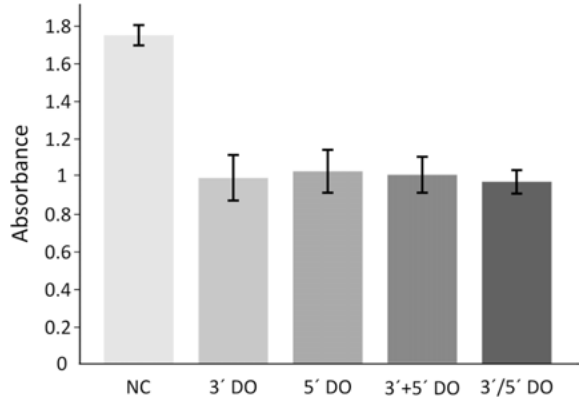

Figure 19: Using different types and combinations of DOs in a single sample does not improve detection. Detection of DNA products and MNPs via UV spectroscopy. 3′ and 5′ represent the two different oligos, discriminated by which end the biotin is at. MNPs used in samples 3′+5′ were functionalized with an equal mix of both oligos. Samples labelled 3′ /5′ contained an equal mix of two pools of MNPs, each with either the 3' or the 5' DO. Error bars represent SD. N=3. Reproduced with permission from Paper III.

6.1.5. Specificity of the assay

The specificity of the recognition of the target by the PLP and the recognition of the products by the MNPs was tested in different papers but reflects the overall robustness of the assay.

In Paper III, a non-complementary PLP was added to the C2CA reaction instead of the complementary one. As seen in Figure 20A, despite the isolation of the correct target by the Dynabeads, samples with the non-complementary PLP showed no difference from the NCs with no target.

In Paper IV, the detection of RCA products involved the use of MNPs functionalized with DOs that were non-complementary to the RCA products, to test the specificity of the binding of MNPs to the products. No significant difference was seen between the NCs and samples containing up to 25 femtomoles of starting target-PLP complexes, which exceeded the LOD by over 30 times.

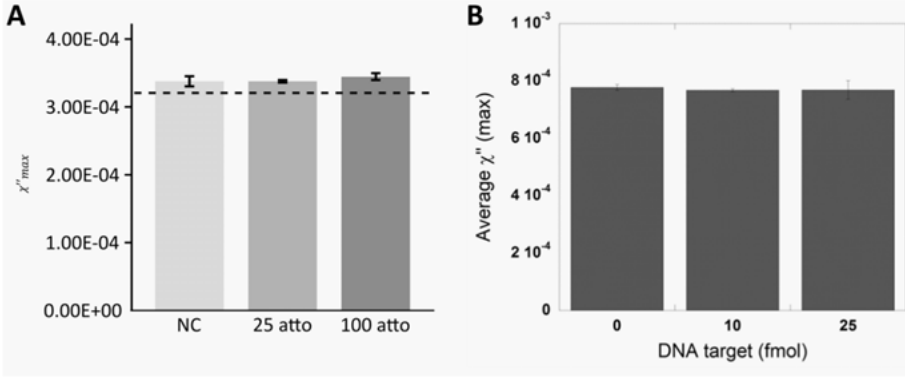

Figure 20: Specificity of the PLPs and DOs. AC susceptometry results from **A:** samples containing 0 (NC), 25, and 100 attomoles of digested plasmid pUUH239.2. Samples underwent C2CA with a non-complementary PLP. The detection was performed using the corresponding DO to the PLP sequence. **B:** Samples detected with MNPs functionalized with a DO non-complementary to the products. Samples with different quantities of the target were amplified using RCA. The dotted line represents the LOD. Error bars represent SD. N=3. Reproduced with permission from Papers III and IV.

The development of the sequence-specific aggregation method is explained in section 6.3, but specificity testing of the aggregation was performed as well. While magnetic particle aggregation has been seen to occur non-specifically[94], the specificity of sequence-specific aggregation was tested in Paper II, by using a non-complementary DO for the RCA products. No aggregation was observed, even at the highest tested target quantity of 20 femtomoles. The results of the AC susceptometry analysis are presented in Figure 21.

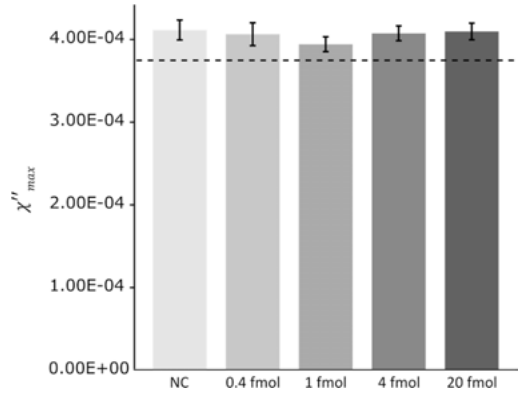

Figure 21: Aggregation does not occur if the DOs used for the functionalization of MNPs cannot bind the RCA products. AC susceptometry results from different samples, where detection of different quantities of RCA products was attempted by adding MNPs with non-complementary DOs to the products. The dotted line represents the LOD. Error bars represent SD. N=3. Reproduced with permission from Paper II.

6.2. Inhibition of phi29 DNA polymerase by digestible ssDNA

6.2.1. Competition between digestion of oligos and polymerization of DNA

While performing various experiments on biological samples, it became clear that there was an unexpected underperformance of phi29 DNA polymerase. Paper V describes the research into this issue, and uncovers a new behaviour of the polymerase. As COs were used for the capture of the target in biological samples, there was a reduction in amplification. This suggested a competition between unbound oligos and extendable 3' ends from the target-PLP complexes. If the quantity of oligos is sufficiently large, the phi29 DNA polymerase digests said oligos before initiating the RCA amplification. Several quantities of ssDNA oligos were added to the reaction mix, and it was observed that the higher the oligo quantity, the lower the amplification, as illustrated in Figure 22.

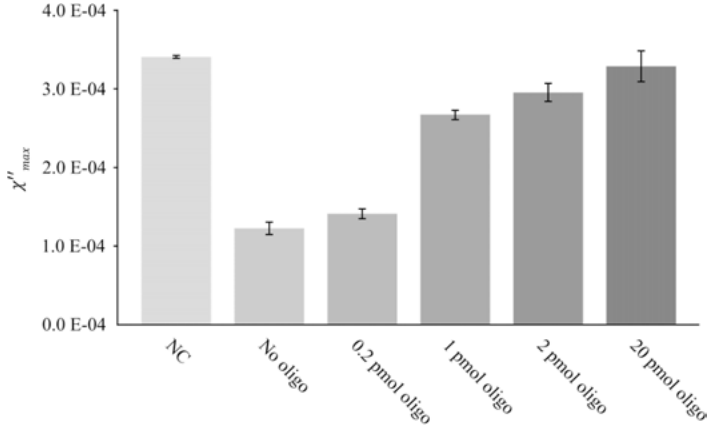

Figure 22: ssDNA oligos hinder the amplification in RCA. An equal starting quantity of target was supplemented with varying quantities of a ssDNA oligo. The more oligo, the less amplification. Error bars represent SD. N=3. Reproduced with permission from Paper V.

6.2.2. Timing of oligo addition and the effect of oligo modifications

It was hypothesized that if there indeed was a competition between oligos and extendable DNA targets, adding oligos after the initiation of the amplification reaction would not reduce the amplification, as phi29 is very processive and will not detach from the template after amplification starts. Another idea was to block the oligos to prevent digestion, either by adding a biotin to their 3' end or incorporating two phosphorothioate bonds at the last two nucleotides

on the 3’ end, preventing cleavage by exonucleases. Both ideas were tested by adding capture oligos at different time points and with different modifications. The results are presented in Figure 23. As can be seen, while the addition of oligos after the start of the polymerization did not hinder the amplification, the modifications on the 3’ ends did not yield any improvement. However, COs perform their function before amplification, and thus, addition after polymerization start was not a viable solution.

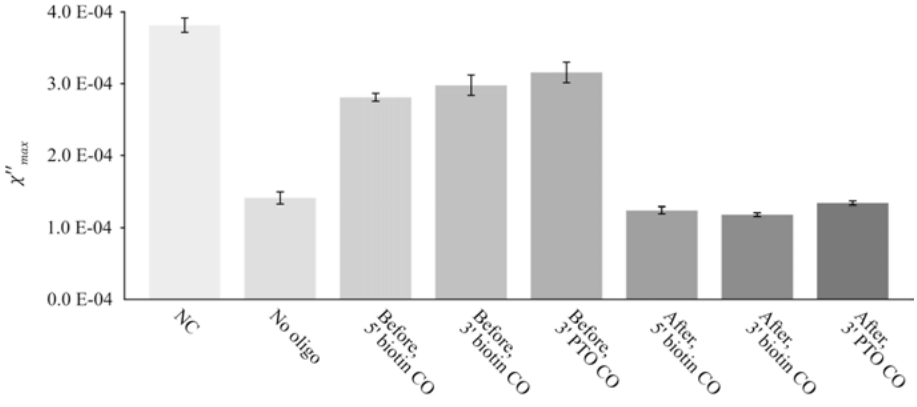

Figure 23: ssDNA oligos competed with an extendable target for binding of phi29 DNA polymerase. The oligos did not hinder amplification when added 90 seconds after the amplification started. However, modifications to stop the digestion of the ssDNA oligos did not rescue the efficiency either. Error bars represent SD. N=3. Reproduced with permission from Paper V.

All findings presented in Paper V point towards a competitive inhibition where phi29 prefers to bind and digest ssDNA rather than extend target-template DNA. In the cases where digestion is not possible due to the modifications, binding still occurs, and the polymerase’s high processivity likely ensures prolonged binding. A schematic representation of the final hypothesis illustrating how the competition between unbound oligos and extendable 3’ ends would affect the amplification can be found in Figure 24. In the absence of a more effective solution, the quantity of COs is reduced in later investigations, such as those in Paper VI. In these experiments, the concentration of COs per sample is reduced 10-fold, from 2 picomoles to 200 femtomoles.

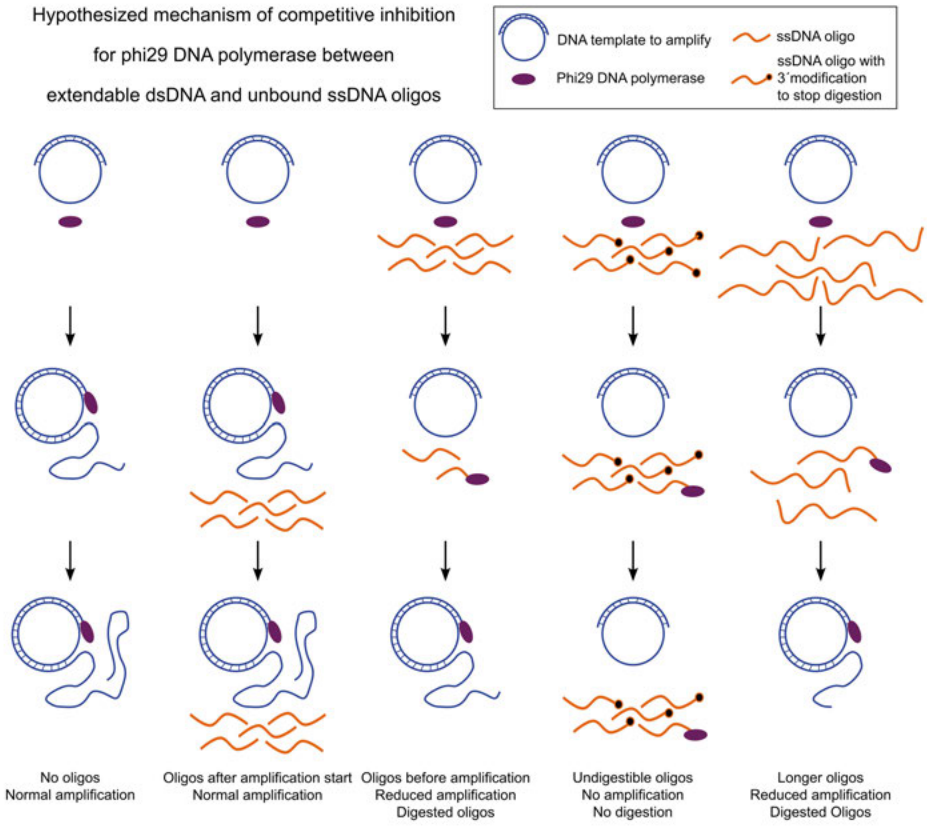

Figure 24: Hypothesized mechanism of competitive inhibition for phi29 DNA polymerase between extendable dsDNA and unbound ssDNA. ssDNA oligos in the amplification reaction are digested preferentially to an extension of the template. However, addition of oligos after amplification start does not hinder the amplification. If the oligos are modified to avoid digestion, the phi29 DNA polymerase will be unable to either digest or detach from the oligos, resulting in the highest inhibition. Longer oligos produce more inhibition than shorter oligos. Reproduced with permission from Paper V.

6.3. Novel detection of products by sequence-specific aggregation

6.3.1. Principle behind sequence-specific aggregation

In Paper II, a novel detection method is described. In the VAM-NDA protocol, the RCA products were usually incubated with functionalized MNPs for 20 minutes at 55 ˚C before detection.[96].

A high-temperature incubation is required for the long ssDNA RCA products to open up and allow the MNPs to bind[78]. Without this incubation step, the binding of MNPs is less effective. However, generally speaking, the binding of complementary sequences is fast. This suggested that the presence of MNPs was not required during the incubation. For this reason, tests were done introducing the MNPs in a more concentrated solution immediately after the heating of the RCA products. This led to the formation of visible clusters and scattered small aggregates. It became clear that if the binding occurred instantaneously and not over time, the addition of MNPs resulted in the collapse and aggregation of the RCA products with the MNPs, resulting in clusters visible to the naked eye. Optimization of this feature followed, exploring the idea that higher temperatures could open the RCA products faster, coupled with a high-salt environment to counteract the negative charges of ssDNA[109] and allow the products to open up in the liquid. Figure 25 shows the optimization of aggregation, testing different temperatures and salt conditions for the incubation after the RCA.

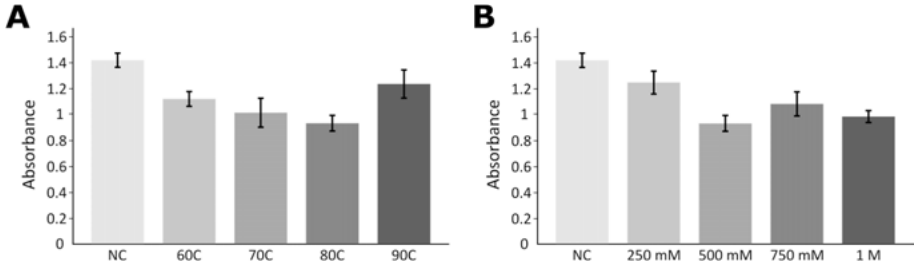

Figure 25: Optimizing aggregation. Absorbance readouts from samples of a single RCA reaction diluted and treated at different temperatures and salt conditions. **A:** Optimization of temperature. **B:** Optimization of NaCl concentration. Error bars represent SD. N=3. Reproduced with permission from Paper II

Optimal conditions were found with temperatures between 70 and 80 ˚C, as well as with NaCl concentrations between 0.5 and 1 M. NaCl concentrations above 1 M have been known to hinder dsDNA formation[110], which is required for the hybridization of the DOs attached to the MNPs and the RCA products. Subsequent tests show that an RCA of 60 minutes, followed by a 20-minute incubation at 80 ˚C with 1 M NaCl, resulted in visible aggregates with starting target quantities as low as 0.4 femtomoles. These samples required no readout instrumentation for qualitative analysis. NaCl also affects DNA aggregation[111], and something that has been a question throughout this thesis is how the aggregates are formed. The addition of the MNPs may form the aggregates, bringing many RCA products together, as one MNP may bind several RCA products. It is however also quite possible that the DNA aggregates partially in a high salt environment on its own, and the addition of MNPs simply allows visualization. Results demonstrate that the binding of MNPs is slightly

more effective using the novel aggregation protocol compared to the traditional VAM-NDA protocol. These findings are presented in Figure 27A and B.

In Paper III, C2CA was performed, followed by the aggregation of the resulting products. The LOD exhibited a 400-fold improvement compared to single RCA detection. For this biological target, a fragment of the resistance gene *sul1* present in the resistance plasmid pUUH239.2[112] (GenBank accession number CP002474.1), could be visually detected in quantities as low as 1 attomole.

Figure 26 displays images, where the aggregates can be seen visually under the microscope, in 96-well plates, and the reaction tubes. Figures 26A and B show aggregates from an RCA reaction, while C shows C2CA results from biological samples. In panels A and B, the samples were spun down for pipetting, and the aggregates are more compact because of this, while in panel C the pictures are taken after aggregation occurs.

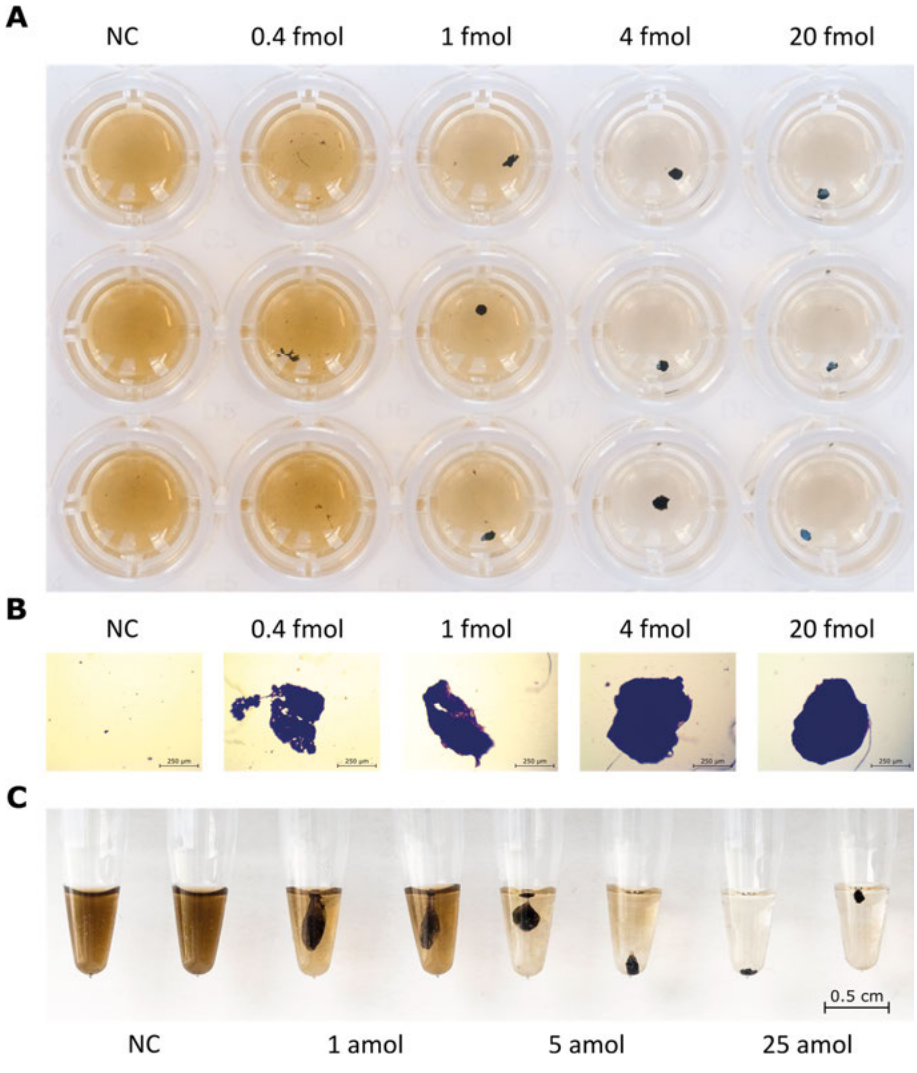

Figure 26: Aggregates formed by sequence-specific aggregation of MNPs and RCA products. **A:** aggregates from RCA products in a 96-well plate. **B:** Representative images of aggregates from panel A imaged under a microscope. **C:** aggregates from C2CA products of a biological target, *sul1*. Reproduced with permission from Papers II and III.

6.3.2. Improvement in detection through sequence-specific aggregation

Following the discovery of the properties of RCA products that facilitated aggregation with functionalized MNPs, important objectives of this thesis included improving, understanding, and using the aggregation phenomenon.

In Paper II, one of the key features is the qualitative visual detection of DNA products. However, given the different appearance of the positive samples compared to the negative samples, alternative quantification methods were explored. AC susceptometry provides valuable information into MNP binding but lacks in readout speed, taking 20 min to measure each sample. [113]. This makes it unideal for diagnostic applications. A shorter analysis was achieved previously by focusing on the frequency points where the maximum observed value of χ''_{max} was for the MNPs, reducing the measurement time to 2 minutes per sample[114]. However, this still required the handling of many samples individually and prolonged analysis for a large batch of samples. For relative quantification, UV spectroscopy can be performed on aggregated samples. Quantification of such samples was feasible due to the dark coloration of the MNPs. Upon aggregating, the solution becomes clearer. This method proved promising as a fast comparative analysis tool for such samples, and this was demonstrated in Paper II. Despite its lower accuracy compared to AC susceptometry because the binding and aggregation do not fully correlate, UV spectroscopy can be used to analyse several samples rapidly, making this technique relevant for clinical samples. In addition, UV-vis spectrophotometers are commonplace in laboratories, facilitating a wider adoption of the sequence-specific aggregation detection method.

While Figure 26A visualizes the aggregates in a 96-well plate, Figure 27 shows the results from AC susceptometry and UV-vis spectroscopy using both the aggregation method and the previous VAM-NDA incubation with the MNPs at 55 ˚C. The results when using the VAM-NDA showed much worse results in UV spectroscopy analysis compared to aggregated samples. UV spectroscopy also provided worse results than AC susceptometry for samples using the aggregation protocol, with the LOD being 1 femtomole instead of 0.4 femtomoles. Regardless, UV-vis is of high value, as it allows much faster analysis of samples.

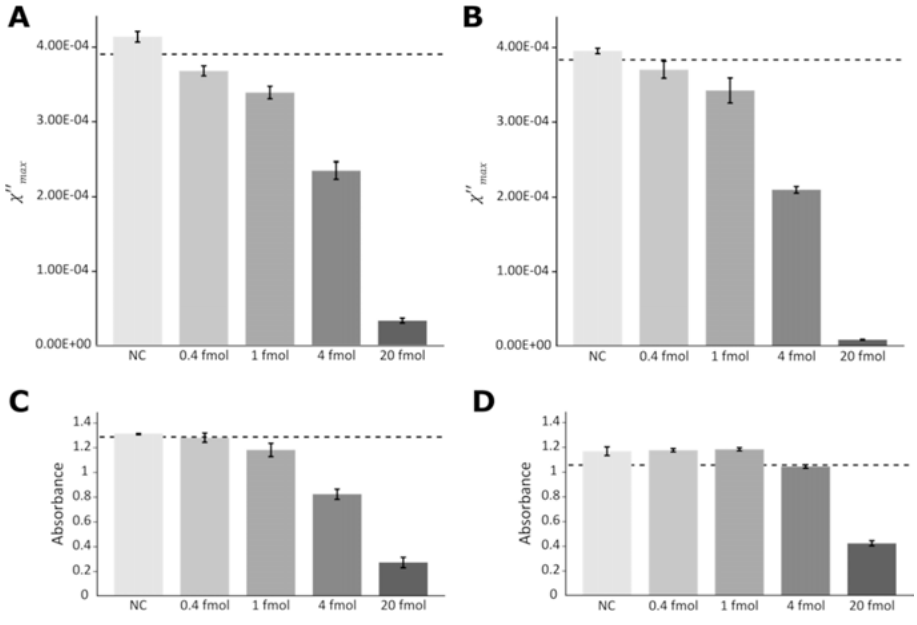

Figure 27: Differences in detection between previous VAM-NDA protocol and sequence-specific aggregation. **A and B:** AC susceptometry results using sequence-specific aggregation and normal VAM-NDA incubation, respectively. **C and D:** absorbance readouts at 350 nm using sequence-specific aggregation and normal VAM-NDA incubation, respectively. The dotted lines represent LOD. Error bars represent SD. N=3. Modified with permission from Paper II.

In Paper III, modifications were made to the aggregation procedure to fit the increased volume and smaller tubes used for C2CA and biological samples. The main improvement involved coupling the incubation to open the RCA products with the inactivation of the polymerase. A single incubation of 5 minutes at 70 ˚C and 0.5 M NaCl proved as reliable as the previous 20-minute incubation. The absence of cooldown to room temperature suggested that the RCA products were already in a semi-open state during amplification, enabling faster preparation for aggregation. A 2-minute 70 ˚C incubation after the addition of MNPs was also included due to the faster cooling of the PCR tubes. Overall, this optimization reduces the aggregation procedure by 15 minutes compared to the VAM-NDA incubation. The visual results can be seen in Figure 26C. This makes the sequence-specific aggregation detection of RCA products a much more viable strategy for POC diagnostics.

6.3.3. Detection of amplification products using coloured polystyrene nanoparticles

After the optimization of the amplification process described in Paper VI, coloured PS-NPs were used for aggregation with the RCA products. These PS-

NPs differ from the MNPs in their composition, being non-magnetic, made of polystyrene, containing a higher amount of streptavidin per particle, and being twice the size, of 200 nm in diameter. Instead of a brown coloration, these PS-NPs contain dyes in red and blue colours.

These coloured PS-NPs showed better aggregation behaviour than the MNPs for visual qualitative analysis, and the visualization of aggregates was considerably easier due to their lighter coloration. However, the lack of AC susceptometry readouts from them makes them less ideal for quantitative studies. Nevertheless, an LOD of 100 zeptomoles was achieved with naked-eye detection. Different quantities of a synthetic target detected with these PS-NPs can be seen in Figure 28.

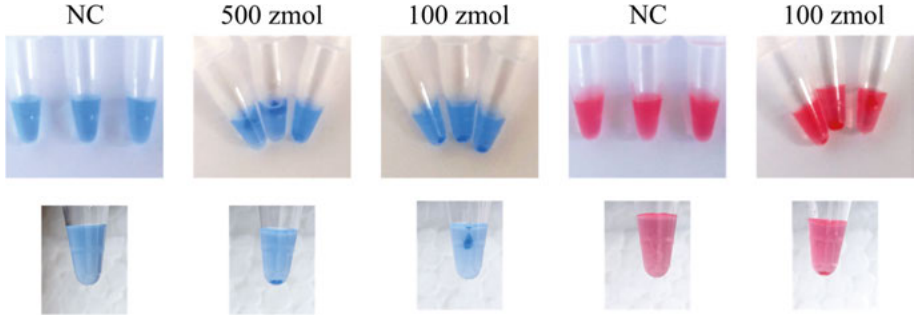

Figure 28: Single target detection using coloured NPs. The top row shows images taken with a smartphone camera, while the bottom row shows pictures taken with a system camera. Reproduced with permission from Paper VI.

6.3.3.1. Multiplexing and image analysis

In Paper VI, both types of coloured PS-NPs were used for multiplex detection of targets in a single sample. Two different synthetic DNA targets, each with different DOs, were amplified using a single C2CA reaction, in a single tube. The aggregation step was slightly modified to ensure proper formation of the first aggregate before introducing the second set of PS-NPs. This modification aimed to prevent subsequent mixing from breaking the already-formed aggregates. This approach allowed for the visual detection of 500 zeptomoles of two different targets within one sample. The results can be seen in Figure 29A.

However, after the aggregation process, it was sometimes challenging to determine whether one or both types of NPs had aggregated. An end-point analysis is of interest, especially with the idea that this bioassay might be performed by a microfluidic chip. Image analysis of the solution's colour shows great promise for this task. Images of the samples were captured with a phone camera using a white balance to facilitate comparisons. ImageJ software was used to split these images into a Lab stack. Single-point measurements of the solution were taken in the A and B channels of the stack. The A and B values were added to yield a total value that correlates with the colour of the solution. Positive values up to 60 indicated red hues, negative values down to -25

represented blue hues, and values around 17 indicated purple hues. The images analysed in this manner and the results of the A+B values are displayed in Figure 29B and C, respectively.

While this method serves as proof of concept, it has some weaknesses, such as the single-point analysis, which can give different values depending on where in the sample the point is selected. However, it provides a foundation for the analysis of the samples, showing a good correlation of A+B with the colour of the solution when using red and blue NPs. In many cases, the results are easily recognizable without the need for such analysis. However, in cases where when the DNA quantity is low and few PS-NPs form aggregates, image analysis could increase the sensitivity of the assay.

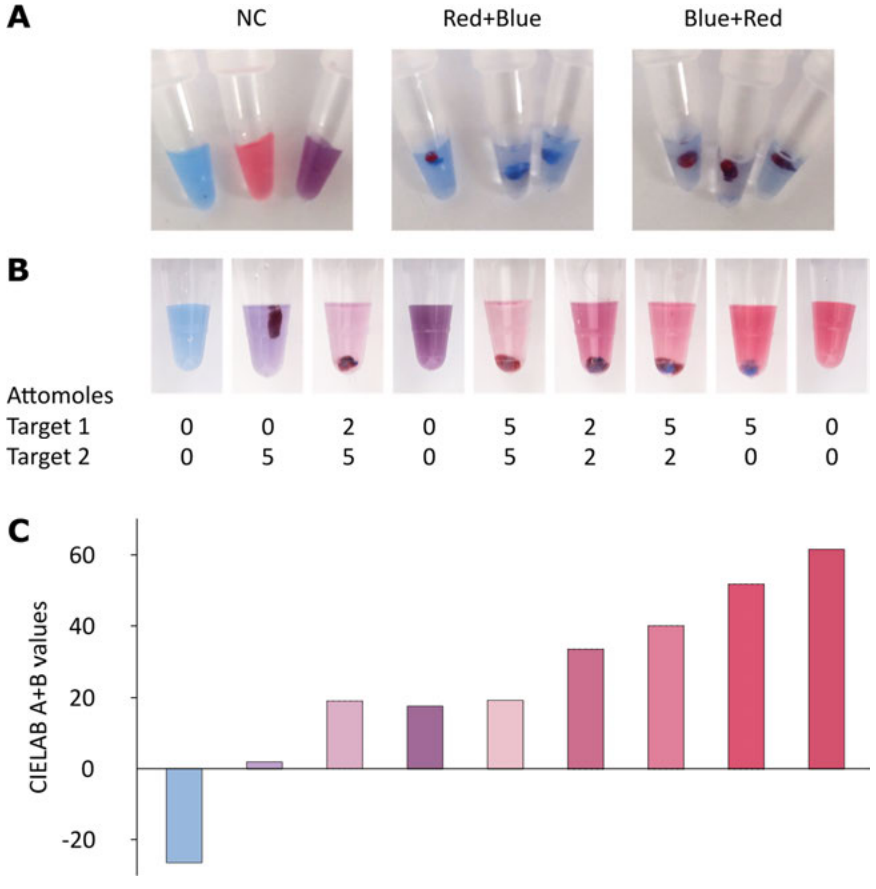

Figure 29: Detection of two targets in one sample. Multiplexing using blue and red NPs. **A:** NCs and 500 zeptomoles of two targets detected by the addition of first red and then blue NPs, or first blue and then red. **B:** Different quantities of two targets to observe the hue of the solutions and the aggregates. Samples with 0 attomoles of both targets as NCs containing only NPs. **C:** Graph showing A+B CIELAB values of the samples in panel B, plotted with each bar matching the colour of the solution. Reproduced with permission from Paper VI.

7. Conclusion and future perspectives

The work presented in this thesis expands on the VAM-NDA technique, moving forward on several fronts to align the method with clinical applications and overcoming certain obstacles toward that goal.

Firstly, optimization has been performed in most steps in the assay. The high sensitivity of VAM-NDA is demonstrated in Papers I and IV. Amplification times have been shortened in those papers and resulted in a highly sensitive magnetic bioassay. Shortening the PLPs also improved the results, especially in C2CA.

The stability of functionalized MNPs, demonstrated in Paper I, proves their long-lasting viability for clinical use. Moreover, all the nanoparticles in this thesis are commercially available, with the PS-NPs presented in Paper VI having a shelf life of 1 year, longer than the 3 months of MNPs.

Optimization of the amplification reactions and reagents across all papers, but mostly Papers V and VI, contribute to cost reduction.

In Paper V, a previously undiscovered feature of phi29 DNA polymerase, a competitive inhibition of the enzyme by ssDNA oligos, was investigated. This is of high importance, as many laboratories use this enzyme with large quantities of oligos in the reaction mix, and there are ways to improve the reactions based on the discovery and results presented in Paper V.

Furthermore, the sequence-specific aggregation detection method, developed in Papers II and III, has been coupled with RCA and C2CA to detect biological samples. This allows for visual detection with sensitivity comparable to VAM-NDA, eliminating the need for read-out instrumentation. This makes this method more attractive to end-users. It even allows the use of common UV-vis spectrophotometers for comparative analysis of samples. Building on that, a visual LOD of 100 zeptomoles was achieved in Paper VI for single samples. A visual LOD of 500 zeptomoles was achieved for multiplexed samples, detecting two targets within one sample.

However, much work remains to be done. The newly discovered features of phi29 described in Paper V complicate the RCA optimization for biological samples. Careful tailoring of phi29 polymerase and oligo quantities is required. Further research on this could improve the sensitivity of the assay.

While visual multiplexed detection has proven viable, issues remain in detection when samples have low DNA target amounts, necessitating more optimization work for clinical settings. The proposed methodology based on

image analysis described in Paper VI could be developed into a simple software to be used in phones, enabling immediate analysis, suitable for point-of-care testing.

A priority for this technology to get into the market in the near future would be the integration of the methodology into a microfluidics chip. This would pose challenges, but the success of integrating other isothermal amplification techniques, including C2CA, suggests the feasibility of the developed method[115,116].

Lastly, basic research into the formation of the aggregates and the behaviour of long ssDNA products under exposure to high heat and high salt conditions could benefit this work, improving the aggregation process and opening new avenues for different detection methods and research areas.

8. Popular summary

Bacterial infections present a common problem and can happen in many different settings, such as homes, hospitals, and outdoor environments. However, treating bacterial infections has become increasingly harder due to the development of antibiotic resistance, where bacteria develop immunity to drugs designed to kill them or inhibit their growth. Bacterial resistance is a growing problem and the lack of new antibiotics further complicates the problem. For this reason, it is extremely important to know if bacteria are resistant to one or another antibiotic before starting treatment.

Unfortunately, the current process for determining resistance is time-consuming, taking days for laboratories to know if the bacteria are resistant to one or several antibiotics. There is a need for tools to detect resistance faster.

Queue in nucleic acid testing! Nearly all forms of antibiotic resistance are given by genes that encode proteins to neutralize the antibiotics. Bacteria can pass genetic elements containing these genes between themselves, leading to the fast spread of resistance. Nucleic acid testing offers a solution by detecting the presence of these genes.

In this thesis, a method for nucleic acid testing has been optimized, bringing it closer to practical application in laboratories, clinics, outbreak settings, or even at home. The technique relies on amplifying specific fragments of genes that produce antibiotic resistance. For this, a technique is used, called rolling circle amplification, that generates long DNA molecules from each fragment, and the larger DNA molecules can then be detected. Nanoparticles that can bind to the DNA molecules are used for detection. In some cases, the nanoparticles used have been magnetic (MNPs), while in others, they were made of polystyrene and dyed with colour (PS-NPs).

In Papers I and IV, MNPs were used for the detection of said products, with a focus on optimization strategies to shorten reaction times. The analysis involves measuring variations in magnetic properties resulting from the binding of the MNPs to the amplification products.

Papers II and III describe a new naked-eye detection method where MNPs form aggregates with amplification products. This method makes interpretation of results easy, with no read-out instrumentation required, as simple eyesight can determine if the samples are positive or negative. The method was proved to be as effective as the magnetic analysis described in Papers I and IV.

Paper V uncovers a mechanism, unknown until now, of a polymerase used to amplify DNA, called phi29 DNA polymerase. This is an enzyme that polymerizes new DNA from a template, and is used around the world for rolling circle amplification. However, it also has a domain to digest DNA that it cannot use as a template. The polymerase has a bias towards this and prioritizes the digestion of DNA over polymerization. These insights have the potential to help researchers in overcoming challenges when using this enzyme, leading to improved test performance

Paper VI showcases improvements in various parts of the assay, such as reducing materials, and using a new polymerase, all of which improved the results. The introduction of red and blue-dyed PS-NPs enhances the detection, resulting in colourful and easy-to-see products. It was also proven that by using these PS-NPs, the detection of two genes in one sample was possible.

In summary, this thesis contributes to the development of existing methods and introduces new approaches for the detection of antibiotic resistance. This brings these methods closer to practical use in laboratories and clinics for the detection of antibiotic resistance. It is very important to say that, while this method has mostly focused on bacterial detection and antibiotic resistance detection, it could easily be used for the detection and characterization of other pathogens. This includes viruses, fungi, and more, in a variety of samples, including water, food, or any other type of sample. The method that provides visual results has great promise for developing a test that provides easily interpretable results, similar to the antigen COVID-19 tests. Lastly, the discovery of interesting behaviour in DNA molecules and proteins opens the door to new and exciting avenues for research in the future.

9. Resumen popular

Las infecciones bacterianas son un problema común y pueden ocurrir en muchos lugares, como en casas, hospitales, o al aire libre. Tratar estas infecciones, sin embargo, solo se convierte en algo más difícil, debido al incremento en la resistencia a antibióticos, las medicinas que se usan para eliminar las bacterias, o parar su crecimiento. La resistencia a antibióticos sigue en aumento y no estamos desarrollando nuevos antibióticos. Por este motivo, es muy importante saber si las bacterias que causan una infección son resistentes a un antibiótico u otro antes de comenzar un tratamiento.

Sin embargo, esto no ocurre frecuentemente. De hecho, pueden pasar días hasta que un laboratorio sepa si las bacterias en una muestra son resistentes a un antibiótico u otro. Necesitamos herramientas para detectar esta resistencia más rápido.

Para ello tenemos los test de ácidos nucleicos. Casi todas las formas de resistencia a antibióticos provienen de genes que las bacterias tienen que producen proteínas para neutralizar a los antibióticos. Los test de ácidos nucleicos ofrecen una solución, detectando directamente la presencia de estos genes.

En esta tesis, un método usado para un test de ácidos nucleicos ha sido optimizado, haciendo que este cerca de poder usarse en laboratorios, clínicas, zonas de brotes de infección, o incluso en casa. Esta técnica se basa en la amplificación de fragmentos de genes. Para ello se ha usado una reacción llamada amplificación por circulo rodante. Después de esta amplificación, en la muestra habrá moléculas de ADN muy largas, que pueden ser detectadas más fácilmente. Esta detección se ha hecho con nanopartículas, en ciertos casos magnéticas y en otros de poliestireno con tintes que les dan color.

En los artículos I y IV, nanopartículas magnéticas se usaron para la detección de los productos, y se optimizaron las reacciones para reducir su duración. Las muestras fueron analizadas con un instrumento que mide si las nanopartículas magnéticas estaban unidas a los productos de la amplificación.

Los artículos II y III describen una nueva técnica donde las nanopartículas forman agregados con los productos de la amplificación. Este nuevo método hace que la interpretación de resultados sea fácil, ya que no requiere instrumentación ya que simple vista vale para saber si las muestras son positivas o negativas. Además, se mejoró la técnica y dio resultados tan buenos visualmente como los de los análisis magnéticos de las muestras en los artículos I y IV.

El articulo V descubre un mecanismo hasta ahora no descrito, de la polimerasa usada para amplificar el ADN. Esta enzima crea nuevo ADN de una cadena molde, y se utiliza en todo el mundo para la replicación pro circulo rodante. Sin embargo, tiene una región dedicada a la digestión de cadenas de ADN que no se puedan usar como molde. LA polimerasa tiene una preferencia por esto, digiriendo el ADN antes de proceder a la polimerización. Estos descubrimientos tienen el potencial de ayudar a muchos investigadores que utilizan esta polimerasa, ayudando a crear tests y métodos con más rendimiento.

En el artículo VI, varias partes de la técnica fueron mejoradas, resultando en el uso de menos materiales, una nueva polimerasa que dio mejores resultados, y otros cambios. También se utilizaron nuevas nanopartículas de colores rojo y azul para la detección, y como consecuencia los resultados son más visuales y fáciles de ver cuando se usan estas nanopartículas. Además, se demostró que detectar dos genes en una sola muestra es posible, usando nanopartículas de diferentes colores.

En conjunto, esta tesis contribuye al desarrollo de métodos ya existentes, e introduce nuevas vías de detección de resistencia a antibióticos. Esto hace que los métodos que se han descrito en estos artículos estén más cerca de poder ser usados en laboratorios y clínicas para la detección de resistencia a antibiótico. Sin embargo, es importante mencionar que, aunque estos métodos y técnicas han sido utilizados para la detección de bacterias y sus resistencias, también se pueden utilizar para la detección de cualquier patógeno que contenga ácidos nucleicos y para la determinación de sus características. Esto puede incluir virus, hongos, etc., y su presencia en agua, comida, u otras muestras. La técnica que produce resultados visuales podría ser usada para desarrollar un test que dé resultados fáciles de interpretar, como el test de antígenos contra la COVID-19. Por último, el comportamiento de varias moléculas y proteínas se han descubierto que podrían llevar a nuevos descubrimientos de alto interés en el futuro.

10. Populärvetenskaplig sammanfattning

Bakteriella infektioner utgör ett vanligt problem som kan förekomma i olika miljöer, inklusive i hemmet, på sjukhus och i utomhusmiljöer. Emellertid har behandlingen av sådana infektioner blivit allt mer utmanande på grund av utvecklingen av antibiotikaresistens, där bakterier utvecklar immunitet mot läkemedel utformade för att döda dem eller hämma deras tillväxt. Den ökande antibiotikaresistensen och bristen på nya antibiotika försvårar situationen ytterligare. Av denna anledning är det viktigt att veta om bakterier är resistenta mot ett eller flera antibiotika innan behandling påbörjas. Den nuvarande processen för att fastställa resistens är tidskrävande, och det kan ta flera dagar för laboratorier att få ett svar. Det finns därför ett påtagligt behov av snabbare diagnostiska verktyg för att upptäcka antibiotikaresistens.

Här kommer nukleinsyratestning in i bilden! Nästan alla former av antibiotikaresistens orsakas av gener som kodar för proteiner som neutraliserar antibiotika. Dessa generna kan överföras mellan bakterier, vilket leder till snabb spridning av resistens. Nukleinsyratestning erbjuder en lösning genom att upptäcka närvaron av dessa gener.

I denna avhandling har en metod för nukleinsyratestning optimerats för att ta oss ett steg närmare praktiska tillämpning, såsom i laboratorier, kliniker, vid sjukdomsutbrott eller till och med i hemmet. Tekniken bygger på amplifiering av specifika genfragment som utvecklar antibiotikaresistens hos bakterier. För detta används den så kallade rullande cirkel-amplifieringen, vilken genererar långa DNA-molekyler från varje fragment. Dessa DNA-molekyler kan sedan detekteras, och för detta ändamål används nanopartiklar som kan binda till dessa molekyler. I detta arbete användes i vissa fall magnetiska nanopartiklar, medan i andra fall användes färgade polystyrenpartiklar.

I artiklarna I och IV användes magnetiska nanopartiklar för detektion av dessa molekyler, med fokus på att optimera olika strategier för att förkorta reaktionstiderna. Analysen involverade mätning av förändringar i magnetiska egenskaper som uppstår på grund av bindningen mellan partiklarna och DNA-produkterna.

De två följande artiklarna (II och III) beskriver en ny metod för visuell detektion, där magnetiska nanopartiklar bildar aggregat med DNA-produkterna. Fördelen med denna metod är att den förenklar tolkningen av resultaten då inget särskilt avläsningsinstrument behövs; det är möjligt att med blotta ögat avgöra om proven är positiva eller negativa. Detektionsmetoden visade sig

vara lika effektiv som den magnetiska analysen som användes i de första två artiklarna.

Artikel V avslöjar en tidigare okänd mekanism hos polymeraset som används för att amplifiera DNA. Detta är ett enzym som polymeriserar nytt DNA utifrån en specifik DNA-sekvens och används över hela världen för rullande cirkel-amplifiering. Polymeraset har visat sig ha en tendens att prioritera nedbrytning av DNA framför polymerisation. Dessa resultat kan vara till hjälp för forskare att övervinna utmaningar i användningen av detta enzym och därigenom förbättra testprestandan

Förbättringar i analysen och användningen av ett nytt polymeras presenteras i artikel VI, vilket resulterade i förbättrade resultat. Användningen av färgade polystyrenpartiklar förbättrade detektionen genom att producera färgglada och synliga DNA-produkter. Dessutom visades det att genom att använda dessa partiklar var det möjligt att detektera två gener i ett och samma prov.

Sammanfattningsvis bidrar denna avhandling till utvecklingen av befintliga metoder och introducerar nya tillvägagångsätt för detektion av antibiotikaresistens. Trots att denna metod har fokuserat på detektion bakterier och antibiotikaresistens, kan den enkelt användas för detektion och karakterisering av andra patogener som virus och svampar i olika typer av prover. Metoden, som ger visuella resultat, har potential för att vidareutveckla ett test som ger lätt tolkbara resultat, liknande antigen COVID-19-testerna.

Slutligen öppnar upptäckten av intressanta beteende hos molekyler och proteiner upp för nya och spännande forskningsområden i framtiden.

11. Acknowledgements

First and foremost, I would like to thank my family for their support and help in this whole endeavor. To my mom, dad and stepmom, because it was not always easy but they always tried to be there and help any way they could. To my brother, for the Sunday calls discussing science, writing, and funny anecdotes. And to the rest of the family, for the much-needed time spent during Christmas holidays in Spain away from the Swedish weather, they were much needed!

Then to my supervisor Teresa, for giving me this chance and for all the help and encouragement regarding courses projects, tricky experiments, posters and presentations, I learned a lot from you. Thank you also for always having an open door and the willingness to discuss any new results or issues. Thank you also to Suparna, it has been great learning from you since my Master´s, and I really appreciate the discussions we had about my PhD and your mentorship efforts. And also of course to my co-supervisor Maria Strømme for her eye for grammar that really improved some of the work here presented!

I would also like to thank all the people I have worked with in these years. Reinier for your sense of humor and fun discussions, it was super cool to learn more of AFM from you. Marie from all the experiments you helped with and performed too, some of this work would not exist otherwise. Linus, for your help in meetings regarding phi29´s work and your calm and positive attitude. Bo, for your insights and discussions on polymerase function, and for the time in South Korea, it was really fun meeting you!

I would also like to thank my colleagues at NFM: Ken, Natalia, Kasper, Christos, Ribooga, Daniel, Michelle, and everyone else who made the group fun to work in. Thank you, Valerie, for being my officemate and keeping the sarcasm level high in the office, all the bad jokes (Hi Ingrid), and the lunches and dinners outside of there too. And also to Anna for the times we spent ranting, but also the fun dinners and cat sharing!

Special thanks too to the AMR people, it was super fun seeing you all at events and sharing science on the topic of antimicrobial resistance. And of course, to Eva for organizing such events and for the great course on science communications that made me want to do better at sharing and presenting science.

Last but not least, thanks to all the friends that have been there during this time, whether in Sweden, Spain, or elsewhere in the world, and that have

supported me or simply made life better with their presence. Special thanks to Petr, living with you was super fun and thank you for all the time discussing the PhD life and for being a poster/presentation sounding board! Thank you Adena as well for the help and encouragement throughout, you always cheered me on. Thank you to Edith for the biosensor discussions and for the time in the conference in South Korea as well. And lastly to Flor, for the endless support and for being the best friend ever.

12. Bibliography

1. Agyeman WY, Bisht A, Gopinath A, Cheema AH, Chaludiya K, Khalid M, Nwosu M, Konka S, Khan S. **(2022)**. A Systematic Review of Antibiotic Resistance Trends and Treatment Options for Hospital-Acquired Multidrug-Resistant Infections. Cureus. 14(10). doi:10.7759/cureus.29956
2. European Council. **(2023)**. Infographic - Five reasons to care about antimicrobial resistance (AMR). https://www.consilium.europa.eu/en/infographics/antimicrobial-resistance/
3. O´Neill J. **(2014)**. Antimicrobial Resistance: Tackling a crisis for the health and wealth of nations. Rev Antimicrob Resist.
4. Vasala A, Hytönen VP, Laitinen OH. **(2020)**. Modern Tools for Rapid Diagnostics of Antimicrobial Resistance. Front Cell Infect Microbiol. 10(July). doi:10.3389/fcimb.2020.00308
5. Heatley NG. **(1944)**. A method for the assay of penicillin. Biochem J. 38(1):61–65. doi:10.1042/bj0380061
6. Balouiri M, Sadiki M, Ibnsouda SK. **(2016)**. Methods for in vitro evaluating antimicrobial activity: A review. J Pharm Anal. 6(2):71–79. doi:10.1016/j.jpha.2015.11.005
7. Nikaido H. **(2009)**. Multidrug Resistance in Bacteria. Annu Rev Biochem. 78(1):119–146. doi:10.1146/annurev.biochem.78.082907.145923
8. Gajic I, Kabic J, Kekic D, Jovicevic M, Milenkovic M, Mitic Culafic D, Trudic A, Ranin L, Opavski N. **(2022)**. Antimicrobial Susceptibility Testing: A Comprehensive Review of Currently Used Methods. Antibiotics. 11(4):1–26. doi:10.3390/antibiotics11040427
9. Bhalla N, Jolly P, Formisano N, Estrela P. **(2016)**. Introduction to biosensors. Essays Biochem. 60(1):1–8. doi:10.1042/EBC20150001
10. Christofi N. **(2005)**. Microbial Tests. In: Worsfold P, Townshend A, Poole C, editors. Encycl Anal Sci. 2nd Editio. New York: Elsevier Ltd; p. 265–271.
11. Gharib G, Bütün İ, Muganlı Z, Kozalak G, Namlı İ, Sarraf SS, Ahmadi VE, Toyran E, van Wijnen AJ, Koşar A. **(2022)**. Biomedical Applications of Microfluidic Devices: A Review. Biosensors. 12(11). doi:10.3390/bios12111023
12. Pierce CP. **(2001)**. Point of Care Testing. BMJ. 322:1285–8. doi:10.1016/B978-0-323-83002-7.00007-3
13. Antoñanzas F, Juárez-Castelló CA, Rodríguez-Ibeas R. **(2021)**. Using point-of-care diagnostic testing for improved antibiotic prescription: an economic model. Health Econ Rev. 11(1):1–12. doi:10.1186/s13561-021-00326-y
14. Spoto G, Corradini R, editors. **(2012)**. Detection of Non-amplified Genomic DNA. New York: Springer. doi:10.1007/978-94-007-1226-3_6
15. Mullis KB. **(1990)**. The Unusual Origin of the Polymerase Chain Reaction. Sci Am. 262(4):56–65. doi:10.1038/scientificamerican0490-56
16. Templeton NS. **(1992)**. The Polymerase Chain Reaction History Methods, and Applications. Diagnostic Mol Pathol. 1(1):58–72.

17. Zhu H, Korabecna M, Neuzil P, Xu Y, Zhang H, Lassakova S. **(2020)**. Review PCR past , present and future. Biotechniques. 69(4):1–9.
18. Garibyan L, Avashia N. **(2013)**. Polymerase Chain Reaction. J Invest Dermatol. 133(3):1–4. doi:10.1038/jid.2013.1
19. Yang S, Rothman RE. **(2004)**. PCR-based diagnostics for infectious diseases: Uses, limitations, and future applications in acute-care settings. Lancet Infect Dis. 4(6):337–348. doi:10.1016/S1473-3099(04)01044-8
20. Zanoli LM, Spoto G. **(2013)**. Isothermal amplification methods for the detection of nucleic acids in microfluidic devices. Biosensors. 3(1):18–43. doi:10.3390/bios3010018
21. Oriero EC, Jacobs J, van Geertruyden JP, Nwakanma D, D'alessandro U. **(2015)**. Molecular-based isothermal tests for field diagnosis of malaria and their potential contribution to malaria elimination. J Antimicrob Chemother. 70(1):2–13. doi:10.1093/jac/dku343
22. Zhao Y, Chen F, Li Q, Wang L, Fan C. **(2015)**. Isothermal Amplification of Nucleic Acids. Chem Rev. 115(22):12491–12545. doi:10.1021/acs.chemrev.5b00428
23. Walker GT, Little MC, Nadeau JG, Shank DD. **(1992)**. Isothermal in vitro amplification of DNA by a restriction enzyme/DNA polymerase system. Proc Natl Acad Sci U S A. 89(1):392–396. doi:10.1073/pnas.89.1.392
24. Liu D, Daubendiek SL, Zillman MA, Ryan K, Kool ET. **(1996)**. Rolling circle DNA synthesis: Small circular oligonucleotides as efficient templates for DNA polymerases. J Am Chem Soc. 118(7):1587–1594. doi:10.1021/ja952786k
25. Fire A, Xu SQ. **(1995)**. Rolling replication of short DNA circles. Proc Natl Acad Sci. 92(10):4641–4645. doi:10.1073/pnas.92.10.4641
26. Notomi T. **(2000)**. Loop-mediated isothermal amplification of DNA. Nucleic Acids Res. 28(12):E63. doi:10.1093/nar/28.12.e63
27. Piepenburg O, Williams CH, Stemple DL, Armes NA. **(2006)**. DNA detection using recombination proteins. PLoS Biol. 4(7):1115–1121. doi:10.1371/journal.pbio.0040204
28. Dean FB, Nelson JR, Giesler TL, Lasken RS. **(2001)**. Rapid amplification of plasmid and phage DNA using Phi29 DNA polymerase and multiply-primed rolling circle amplification. Genome Res. 11(6):1095–1099. doi:10.1101/gr.180501
29. Subkhankulova T, Livesey FJ. **(2006)**. Comparative evaluation of linear and exponential amplification techniques for expression profiling at the single-cell level. Genome Biol. 7(3). doi:10.1186/gb-2006-7-3-r18
30. Cheng Y, Zhang X, Li Z, Jiao X, Wang Y, Zhang Y. **(2009)**. Highly sensitive determination of microrna using target-primed and branched rolling-circle amplification. Angew Chemie - Int Ed. 48(18):3268–3272. doi:10.1002/anie.200805665
31. Sun J, de Hoog S. **(2013)**. Hyperbranching Rolling Circle Amplification, An Improved Protocol for Discriminating Between Closely Related Fungal Species. In: Fungal Diagnostics. New York: Springer; p. 167–175. doi:10.1007/978-1-62703-257-5_13
32. Goo NI, Kim DE. **(2016)**. Rolling circle amplification as isothermal gene amplification in molecular diagnostics. Biochip J. 10(4):262–271. doi:10.1007/s13206-016-0402-6

33. Kumari R, Lim JW, Sullivan MR, Malampy R, Baush C, Smolina I, Robin H, Demidov V V., Ugolini GS, Auclair JR, Konry T. **(2022)**. A Novel Rolling Circle Amplification-Based Detection of SARS-CoV-2 with Multi-Region Padlock Hybridization. Diagnostics. 12(9):1–11. doi:10.3390/diagnostics12092252
34. Gu L, Yan W, Liu L, Wang S, Zhang X, Lyu M. **(2018)**. Research progress on rolling circle amplification (Rca)-based biomedical sensing. Pharmaceuticals. 11(2):1–19. doi:10.3390/ph11020035
35. Nilsson M, Malmgren H, Samiotaki M, Kwiatkowski M, Chowdhary BP, Landegren U. **(1994)**. Padlock probes: Circularizing oligonucleotides for localized DNA detection. Science (80-). 265(5181):2085–2088. doi:10.1126/science.7522346
36. Lizardi PM, Huang X, Zhu Z, Bray-Ward P, Thomas DC, Ward DC. **(1998)**. Mutation detection and single-molecule counting using isothermal rolling-circle amplification. Nat Genet. 19(3):225–232. doi:10.1038/898
37. Edwards KJ, Reid AL, Coghill JA, Berry ST, Barker GLA. **(2009)**. Multiplex single nucleotide polymorphism (SNP)-based genotyping in allohexaploid wheat using padlock probes. Plant Biotechnol J. 7(4):375–390. doi:10.1111/j.1467-7652.2009.00413.x
38. Blanco L, Bernad A, Lázaro JM, Martín G, Garmendia C, Salas M. **(1989)**. Highly Efficient DNA Synthesis by the Phage ϕ 29 DNA Polymerase. J Biol Chem. 264(15):8935–8940. doi:10.1016/s0021-9258(18)81883-x
39. Berman AJ, Kamtekar S, Goodman JL, Lázaro JM, De Vega M, Blanco L, Salas M, Steitz TA. **(2007)**. Structures of phi29 DNA polymerase complexed with substrate: The mechanism of translocation in B-family polymerases. EMBO J. 26(14):3494–3505. doi:10.1038/sj.emboj.7601780
40. del Prado A, Rodríguez I, Lázaro JM, Moreno-Morcillo M, de Vega M, Salas M. **(2019)**. New insights into the coordination between the polymerization and 3′-5′ exonuclease activities in ϕ29 DNA polymerase. Sci Rep. 9(1):1–13. doi:10.1038/s41598-018-37513-7
41. Esteban JA, Salas M, Blanco L. **(1993)**. Fidelity of φ29 DNA polymerase. Comparison between protein-primed initiation and DNA polymerization. J Biol Chem. 268(4):2719–2726. doi:10.1016/s0021-9258(18)53833-3
42. Dahl F, Banér J, Gullberg M, Mendel-Hartvig M, Landegren U, Nilsson M. **(2004)**. Circle-to-circle amplification for precise and sensitive DNA analysis. Proc Natl Acad Sci U S A. 101(13):4548–4553. doi:10.1073/pnas.0400834101
43. Ciftci S, Neumann F, Hernández-Neuta I, Hakhverdyan M, Bálint Á, Herthnek D, Madaboosi N, Nilsson M. **(2019)**. A novel mutation tolerant padlock probe design for multiplexed detection of hypervariable RNA viruses. Sci Rep. 9(1):1–10. doi:10.1038/s41598-019-39854-3
44. Zakeri H, Shokohi T, Badali H, Mayahi S, Didehdar M. **(2015)**. Use of padlock probes and rolling circle amplification (RCA) for rapid identification of trichophyton species, related to human and animal disorder. Jundishapur J Microbiol. 8(7). doi:10.5812/jjm.19107v2
45. Jain S, Dandy DS, Geiss BJ, Henry CS. **(2021)**. Padlock probe-based rolling circle amplification lateral flow assay for point-of-need nucleic acid detection. Analyst. 146(13):4340–4347. doi:10.1039/D1AN00399B
46. Barreto SC, Uppalapati M, Ray A. **(2014)**. Small circular DNAs in human pathology. Malaysian J Med Sci. 21(3):4–18.

47. Yang L, Jia R, Ge T, Ge S, Zhuang A, Chai P, Fan X. **(2022)**. Extrachromosomal circular DNA: biogenesis, structure, functions and diseases. Signal Transduct Target Ther. 7(1):1–21. doi:10.1038/s41392-022-01176-8
48. Ulanovsky L, Bodner M, Trifonov EN, Choder M. **(1986)**. Curved DNA: Design, synthesis, and circularization. Proc Natl Acad Sci U S A. 83(4):862–866. doi:10.1073/pnas.83.4.862
49. Frieden M, Pedroso E, Kool ET. **(1999)**. Tightening the belt on polymerases: Evaluating the physical constraints on enzyme substrate size. Angew Chemie - Int Ed. 38(24):3654–3657. doi:10.1002/(SICI)1521-3773(19991216)38:24<3654::AID-ANIE3654>3.0.CO;2-S
50. Mills A, Gago F. **(2021)**. Structural landscape of the transition from an ssdna dumbbell plus its complementary hairpin to a dsdna microcircle via a kissing loop intermediate. Molecules. 26(10). doi:10.3390/molecules26103017
51. Joffroy B, Uca YO, Prešern D, Doye JPK, Schmidt TL. **(2018)**. Rolling circle amplification shows a sinusoidal template length-dependent amplification bias. Nucleic Acids Res. 46(2):538–545. doi:10.1093/nar/gkx1238
52. Morin JA, Cao FJ, Lázaro JM, Arias-Gonzalez JR, Valpuesta JM, Carrascosa JL, Salas M, Ibarra B. **(2012)**. Active DNA unwinding dynamics during processive DNA replication. Proc Natl Acad Sci U S A. 109(21):8115–8120. doi:10.1073/pnas.1204759109
53. Garbarino F, Minero GAS, Rizzi G, Fock J, Hansen MF. **(2019)**. Integration of rolling circle amplification and optomagnetic detection on a polymer chip. Biosens Bioelectron. 142(April):111485. doi:10.1016/j.bios.2019.111485
54. Minero GAS, Fock J, Tian B, Rizzi G, Neumann F, Madaboosi N, Nilsson M, Fougt Hansen M. **(2020)**. Real-time analysis of switchable nanocomposites of magnesium pyrophosphates and rolling circle amplification products. ChemNanoMat. 6(8):1276–1282. doi:10.1002/cnma.202000135
55. Southern EM. **(1975)**. Detection of specific sequences among DNA fragments separated by gel electrophoresis. 1975. Biotechnology. 24:122–139. doi:10.1016/b978-0-12-131200-8.50041-1
56. Saiki RK, Scharf S, Faloona F, Mullis KB, Horn GT, Erlich HA, Arnheim N. **(1985)**. Enzymatic amplification of beta-globin genomic sequences and restriction site analysis for diagnosis of sickle cell anemia. 1985. Biotechnology. 24:476–480.
57. Borst P. **(2005)**. Ethidium DNA agarose gel electrophoresis: How it started. IUBMB Life. 57(11):745–747. doi:10.1080/15216540500380855
58. Bogiel T, Mikucka A, Kanarek P. **(2022)**. Agarose Gel Electrophoresis-Based RAPD-PCR—An Optimization of the Conditions to Rapidly Detect Similarity of the Alert Pathogens for the Purpose of Epidemiological Studies. Gels. 8(12). doi:10.3390/gels8120760
59. Chen M, He Q, Tong Y, Chen Z. **(2021)**. A universal fluorescent sensing system for pathogen determination based on loop-mediated isothermal amplification triggering dual-primer rolling circle extension. Sensors Actuators, B Chem. 331(January):129436. doi:10.1016/j.snb.2021.129436
60. Larsson C, Grundberg I, Söderberg O, Nilsson M. **(2010)**. In situ detection and genotyping of individual mRNA molecules. Nat Methods. 7(5):395–397. doi:10.1038/nmeth.1448

61. Clausson CM, Arngården L, Ishaq O, Klaesson A, Kühnemund M, Grannas K, Koos B, Qian X, Ranefall P, Krzywkowski T, et al. **(2015)**. Compaction of rolling circle amplification products increases signal integrity and signal-to-noise ratio. Sci Rep. 5(March):1–10. doi:10.1038/srep12317
62. Russel H, Carita F, Gavin D, Robert W. **(1993)**. Kinetic PCR Analysis: Real-time Monitoring of DNA Amplification Reactions. Biotechnology. 11:1026–1030. http://www.nature.com/naturebiotechnology
63. Zuo X, Xia F, Xiao Y, Plaxco KW. **(2010)**. Sensitive and Selective Amplified Fluorescence DNA Detection Based on Exonuclease III-Aided Target Recycling. J Am Chem Soc. 132(6):1816–1818. doi:10.1021/ja909551b
64. Llandro J, Palfreyman JJ, Ionescu A, Barnes CHW. **(2010)**. Magnetic biosensor technologies for medical applications: A review. Med Biol Eng Comput. 48(10):977–998. doi:10.1007/s11517-010-0649-3
65. Li Y, Cheng H, Alhalili Z, Xu G, Gao G. **(2021)**. The progress of magnetic sensor applied in biomedicine: A review of non-invasive techniques and sensors. J Chinese Chem Soc. 68(2):216–227. doi:10.1002/jccs.202000353
66. Chen Y, Ding X, Zhang Y, Natalia A, Sun X, Wang Z, Shao H. **(2018)**. Design and synthesis of magnetic nanoparticles for biomedical diagnostics. Quant Imaging Med Surg. 8(9):957–970. doi:10.21037/qims.2018.10.07
67. Abarca-Cabrera L, Fraga-García P, Berensmeier S. **(2021)**. Bio-nano interactions: binding proteins, polysaccharides, lipids and nucleic acids onto magnetic nanoparticles. Biomater Res. 25(1):1–18. doi:10.1186/s40824-021-00212-y
68. Hall EH. **(1879)**. On a New Action of the Magnet on Electric Currents. Am J Math. 2(3):287. doi:10.2307/2369245
69. Fan H, Wang J, Feng Q, Hu Q, Zuo S, Nabaei V, Heidari H. **(2021)**. Detection techniques of biological and chemical Hall sensors. RSC Adv. 11(13):7257–7270. doi:10.1039/d0ra10027g
70. Wang SX, Li G. **(2008)**. Advances in giant magnetoresistance biosensors with magnetic nanpparticle tags: Review and outlook. IEEE Trans Magn. 44(7):1687–1702. doi:10.1109/TMAG.2008.920962
71. Vázquez M, Knobel M, Sánchez ML, Valenzuela R, Zhukov AP. **(1997)**. Giant magnetoimpedance effect in soft magnetic wires for sensor applications. Sensors Actuators, A Phys. 59(1–3):20–29. doi:10.1016/S0924-4247(97)80143-4
72. Jimenez VO, Hwang KY, Nguyen D, Rahman Y, Albrecht C, Senator B, Thiabgoh O, Devkota J, Bui VDA, Lam DS, et al. **(2022)**. Magnetoimpedance Biosensors and Real-Time Healthcare Monitors: Progress, Opportunities, and Challenges. Biosensors. 12(7):517. doi:10.3390/bios12070517
73. Xianyu Y, Wang Q, Chen Y. **(2018)**. Magnetic particles-enabled biosensors for point-of-care testing. TrAC - Trends Anal Chem. 106:213–224. doi:10.1016/j.trac.2018.07.010
74. Debye P. **(1929)**. Polar Molecules. New York: The Chemical Catalogue Company. doi:https://onlinelibrary.wiley.com/doi/10.1002/jctb.5000484320
75. Erne BH, Butter K, Kuipers BWM, Vroege GJ. **(2003)**. Rotational Diffusion in Iron Ferrofluids. :8218–8225.
76. Connolly J, St Pierre TG. **(2001)**. Proposed biosensors based on time-dependent properties of magnetic fluids. J Magn Magn Mater. 225(1–2):156–160. doi:10.1016/S0304-8853(00)01245-2

77. Astalan AP, Ahrentorp F, Johansson C, Larsson K, Krozer A. **(2004)**. Biomolecular reactions studied using changes in Brownian rotation dynamics of magnetic particles. Biosens Bioelectron. 19(8):945–951. doi:10.1016/j.bios.2003.09.005
78. Strömberg M, Göransson J, Gunnarsson K, Nilsson M, Svedlindh P, Strømme M. **(2008)**. Sensitive molecular diagnostics using volume-amplified magnetic nanobeads. Nano Lett. 8(3):816–821. doi:10.1021/nl072760e
79. Tataurov A V., You Y, Owczarzy R. **(2008)**. Predicting ultraviolet spectrum of single stranded and double stranded deoxyribonucleic acids. Biophys Chem. 133(1–3):66–70. doi:10.1016/j.bpc.2007.12.004
80. Baptista P V., Koziol-Montewka M, Paluch-Oles J, Doria G, Franco R. **(2006)**. Gold-Nanoparticle-Probe–Based Assay for Rapid and Direct Detection of Mycobacterium tuberculosis DNA in Clinical Samples. Clin Chem. 52(7):1433–1434. doi:10.1373/clinchem.2005.065391
81. Nguyen HH, Park J, Kang S, Kim M. **(2015)**. Surface Plasmon Resonance: A Versatile Technique for Biosensor Applications. :10481–10510. doi:10.3390/s150510481
82. Huang X, El-sayed MA. **(2010)**. Gold nanoparticles : Optical properties and implementations in cancer diagnosis and photothermal therapy. :13–28. doi:10.1016/j.jare.2010.02.002
83. Li J, Deng T, Chu X, Yang R, Jiang J, Shen G, Yu R. **(2010)**. Rolling circle amplification combined with gold nanoparticle aggregates for highly sensitive identification of single-nucleotide polymorphisms. Anal Chem. 82(7):2811–2816. doi:10.1021/ac100336n
84. Liu P, Yang X, Sun S, Wang Q, Wang K, Huang J, Liu J, He L. **(2013)**. Enzyme-free colorimetric detection of DNA by using gold nanoparticles and hybridization chain reaction amplification. Anal Chem. 85(16):7689–7695. doi:10.1021/ac4001157
85. Li H, Rothberg LJ. **(2004)**. Label-free colorimetric detection of specific sequences in genomic DNA amplified by the polymerase chain reaction. J Am Chem Soc. 126(35):10958–10961. doi:10.1021/ja048749n
86. Wachiralurpan S, Sriyapai T, Areekit S, Sriyapai P, Augkarawaritsawong S, Santiwatanakul S, Chansiri K. **(2018)**. Rapid Colorimetric Assay for Detection of Listeria monocytogenes in Food Samples Using LAMP Formation of DNA Concatemers and Gold Nanoparticle-DNA Probe Complex. Front Chem. 6(April):1–9. doi:10.3389/fchem.2018.00090
87. Fischbach J, Loh Q, Bier FF, Lim TS, Frohme M, Glökler J. **(2017)**. Alizarin Red S for Online Pyrophosphate Detection Identified by a Rapid Screening Method. Sci Rep. 7(November 2016):1–9. doi:10.1038/srep45085
88. Tang W, Zhang M, Yue T, Wang X, Li Z. **(2021)**. Low-cost colorimetric reader and label-free strategy for user-friendly detection of nucleic acid amplification products. Sensors Actuators B Chem. 346(June):130523. doi:10.1016/j.snb.2021.130523
89. Tanner NA, Zhang Y, Evans TC. **(2015)**. Visual detection of isothermal nucleic acid amplification using pH-sensitive dyes. Biotechniques. 58(2):59–68. doi:10.2144/000114253
90. Goto M, Honda E, Ogura A, Nomoto A, Hanaki KI. **(2009)**. Colorimetric detection of loop-mediated isothermal amplification reaction by using hydroxy naphthol blue. Biotechniques. 46(3):167–172. doi:10.2144/000113072

91. Zhang Y, Hunt EA, Tamanaha E, Corrêa IR, Tanner NA. **(2022)**. Improved visual detection of DNA amplification using pyridylazophenol metal sensing dyes. Commun Biol. 5(1):1–9. doi:10.1038/s42003-022-03973-x
92. Jarvius J, Melin J, Göransson J, Stenberg J, Fredriksson S, Gonzalez-Rey C, Bertilsson S, Nilsson M. **(2006)**. Digital quantification using amplified single-molecule detection. Nat Methods. 3(9):725–727. doi:10.1038/nmeth916
93. Jiang HX, Liang ZZ, Ma YH, Kong DM, Hong ZY. **(2016)**. G-quadruplex fluorescent probe-mediated real-time rolling circle amplification strategy for highly sensitive microRNA detection. Anal Chim Acta. 943:114–122. doi:10.1016/j.aca.2016.09.019
94. Lin C, Zhang Y, Zhou X, Yao B, Fang Q. **(2013)**. Naked-eye detection of nucleic acids through rolling circle amplification and magnetic particle mediated aggregation. Biosens Bioelectron. 47:515–519. doi:10.1016/j.bios.2013.03.056
95. Akhtar S, Strömberg M, Zardán Gómez De La Torre T, Russell C, Gunnarsson K, Nilsson M, Svedlindh P, Strømme M, Leifer K. **(2010)**. Real-space transmission electron microscopy investigations of attachment of functionalized magnetic nanoparticles to DNA-coils acting as a biosensor. J Phys Chem B. 114(41):13255–13262. doi:10.1021/jp105756b
96. Oropesa-Nuñez R, Zardán Gómez De La Torre T, Stopfel H, Svedlindh P, Strömberg M, Gunnarsson K. **(2020)**. Insights into the Formation of DNA-Magnetic Nanoparticle Hybrid Structures: Correlations between Morphological Characterization and Output from Magnetic Biosensor Measurements. ACS Sensors. 5(11):3510–3519. doi:10.1021/acssensors.0c01623
97. Intarapanich A, Kaewkamnerd S, Shaw PJ, Ukosakit K, Tragoonrung S, Tongsima S. **(2015)**. Automatic DNA Diagnosis for 1D Gel Electrophoresis Images using Bio-image Processing Technique. BMC Genomics. 16(12):1–11. doi:10.1186/1471-2164-16-S12-S15
98. Spata MO, Castagna ME, Conoci S. **(2015)**. Image data analysis in qPCR: A method for smart analysis of DNA amplification. Sens Bio-Sensing Res. 6:79–84. doi:10.1016/j.sbsr.2015.10.006
99. Osinski BL, BenTaieb A, Ho I, Jones RD, Joshi RP, Westley A, Carlson M, Willis C, Schleicher L, Mahon BM, Stumpe MC. **(2022)**. Artificial intelligence-augmented histopathologic review using image analysis to optimize DNA yield from formalin-fixed paraffin-embedded slides. Mod Pathol. 35(12):1791–1803. doi:10.1038/s41379-022-01161-0
100. Schneider CA, Rasband WS, Eliceiri KW. **(2012)**. NIH Image to ImageJ: 25 years of image analysis. Nat Methods. 9(7):671–675. doi:10.1038/nmeth.2089
101. Abràmoff MD, Magalhães PJ, Ram SJ. **(2004)**. Image processing with imageJ. Biophotonics Int. 11(7):36–41. doi:10.1201/9781420005615.ax4
102. Blab GA, Schmidt T, Nilsson M. **(2004)**. Homogeneous Detection of Single Rolling Circle Replication Products. Anal Chem. 76(2):495–498. doi:10.1021/ac034987+
103. Zardán Gómez De La Torre T, Strömberg M, Russell C, Göransson J, Nilsson M, Svedlindh P, Strømme M. **(2010)**. Investigation of immobilization of functionalized magnetic nanobeads in rolling circle amplified DNA coils. J Phys Chem B. 114(10):3707–3713. doi:10.1021/jp911251k

104. Strömberg M, Zardán Gómez de la Torre T, Nilsson M, Svedlindh P, Strømme M. **(2014)**. A magnetic nanobead-based bioassay provides sensitive detection of single- and biplex bacterial DNA using a portable AC susceptometer. Biotechnol J. 9(1):137–145. doi:10.1002/biot.201300348
105. Bejhed RS, Zardán Gómez De La Torre T, Donolato M, Hansen MF, Svedlindh P, Strömberg M. **(2015)**. Turn-on optomagnetic bacterial DNA sequence detection using volume-amplified magnetic nanobeads. Biosens Bioelectron. 66:405–411. doi:10.1016/j.bios.2014.11.048
106. Engström A, Zardán Gómez de la Torre T, Strømme M, Nilsson M, Herthnek D. **(2013)**. Detection of Rifampicin Resistance in Mycobacterium tuberculosis by Padlock Probes and Magnetic Nanobead-Based Readout. PLoS One. 8(4). doi:10.1371/journal.pone.0062015
107. Sepehri S, Zardán Gómez De La Torre T, Schneiderman JF, Blomgren J, Jesorka A, Johansson C, Nilsson M, Albert J, Strømme M, Winkler D, Kalaboukhov A. **(2019)**. Homogeneous Differential Magnetic Assay. ACS Sensors. 4(9):2381–2388. doi:10.1021/acssensors.9b00969
108. Tian B, Fock J, Minero GAS, Garbarino F, Hansen MF. **(2019)**. Ultrasensitive Real-Time Rolling Circle Amplification Detection Enhanced by Nicking-Induced Tandem-Acting Polymerases. Anal Chem. 91(15):10102–10109. doi:10.1021/acs.analchem.9b02073
109. Tan ZJ, Chen SJ. **(2006)**. Nucleic acid helix stability: Effects of salt concentration, cation valence and size, and chain length. Biophys J. 90(4):1175–1190. doi:10.1529/biophysj.105.070904
110. Tomac S, Sarkar M, Ratilainen T, Wittung P, Nielsen PE, Norden B, Graslund A. **(1996)**. Ionic effects on the stability and conformation of peptide nucleic acid complexes. J Am Chem Soc. 118(24):5544–5552. doi:10.1021/ja9604951
111. Kawakita H, Uneyama T, Kojima M, Morishima K, Masubuchi Y, Watanabe H. **(2009)**. Formation of globules and aggregates of DNA chains in DNA/polyethylene glycol/monovalent salt aqueous solutions. J Chem Phys. 131(9). doi:10.1063/1.3216110
112. Sandegren L, Linkevicius M, Lytsy B, Melhus Å, Andersson DI. **(2012)**. Transfer of an Escherichia coli ST131 multiresistance cassette has created a Klebsiella pneumoniae-specific plasmid associated with a major nosocomial outbreak. J Antimicrob Chemother. 67(1):74–83. doi:10.1093/jac/dkr405
113. de la Torre TZG, Mezger A, Herthnek D, Johansson C, Svedlindh P, Nilsson M, Strømme M. **(2011)**. Detection of rolling circle amplified DNA molecules using probe-tagged magnetic nanobeads in a portable AC susceptometer. Biosens Bioelectron. 29(1):195–199. doi:10.1016/j.bios.2011.08.019
114. De La Torre TZG, Herthnek D, Strømme M. **(2017)**. A magnetic nanobead-based read-out procedure for rapid detection of DNA molecules. J Nanosci Nanotechnol. 17(4):2861–2864. doi:10.1166/jnn.2017.13877
115. Kühnemund M, Witters D, Nilsson M, Lammertyn J. **(2014)**. Circle-to-circle amplification on a digital microfluidic chip for amplified single molecule detection. Lab Chip. 14(16):2983–2992. doi:10.1039/c4lc00348a
116. Zhang H, Xu Y, Fohlerova Z, Chang H, Iliescu C, Neuzil P. **(2019)**. LAMP-on-a-chip: Revising microfluidic platforms for loop-mediated DNA amplification. TrAC - Trends Anal Chem. 113(January):44–53. doi:10.1016/j.trac.2019.01.015

Acta Universitatis Upsaliensis

Digital Comprehensive Summaries of Uppsala Dissertations from the Faculty of Science and Technology 2362

Editor: The Dean of the Faculty of Science and Technology

A doctoral dissertation from the Faculty of Science and Technology, Uppsala University, is usually a summary of a number of papers. A few copies of the complete dissertation are kept at major Swedish research libraries, while the summary alone is distributed internationally through the series Digital Comprehensive Summaries of Uppsala Dissertations from the Faculty of Science and Technology. (Prior to January, 2005, the series was published under the title "Comprehensive Summaries of Uppsala Dissertations from the Faculty of Science and Technology".)

Distribution: publications.uu.se
urn:nbn:se:uu:diva-522171

ACTA UNIVERSITATIS
UPSALIENSIS
2024